INTERNATIONAL ATOMIC ENERGY AGENCY
UNITED NATIONS EDUCATIONAL, SCIENTIFIC AND CULTURAL ORGANIZATION
INTERNATIONAL CENTRE FOR THEORETICAL PHYSICS
I.C.T.P., P.O. BOX 586, 34100 TRIESTE, ITALY, CABLE: CENTRATOM TRIESTE

H4.SMR/638-6

College on Medical Physics: Imaging and Radiation Protection

31 August - 18 September 1992

Nuclear Detectors and Electronics

R. Cesareo

Centro per l'Ingegneria Biomedica
Università di Roma,"La Sapienza"
Rome, Italy &
Istituto di Matematica Fisica
Università di Sassari,
Sassari, Italy

College on Medical Physics
Imaging and Radiation Protection

31 August - 18 September 1992

NUCLEAR DETECTORS AND ELECTRONICS

Roberto CESAREO, Centro per l'Ingegneria Biomedica, Universita' di Roma "La Sapienza" , Rome, Italy and Istituto di Matematica e
Fisica, Universita' di Sassari, Sassari, Italy

INDEX

1. INTRODUCTION

The detection of charged particles (alpha, protons, electrons and so on) of neutrons and of ionizing radiation (X and gamma rays) is based on their property of directly or indirectly ionizing as it passes through matter. Charged particles ionize directly and this process is described by the Bethe-Bloch equation giving the stopping power of charged particles versus energy (Section 2).
Ionizing radiation, like X or gamma rays interact with matter mainly through: a)photoelectric effect; b)Compton scattering; c)Rayleigh scattering; d)pair production. As a consequence of the effects a) and b) electrons are produced, and of the effect d)a pair of electron-positron, which ionize the matter as charged particles (Section 3).
Also neutrons are not directly ionizing, and can be detected indirectly through the following effects: a) collision with a nucleus; b)nuclear reactions; and c)nuclear fission, which all give rise to heavy charged particles which ionize the matter (Section 4).
The different types of detectors and their characteristics are then described in Section 5, including gas detectors (ionization chambers, gas proportional detectors, Geiger-Muller and position-sensitive detectors), scintillation detectors and semiconductor detectors (cooled and room-temperature).
The Electronics is then described in Section 6, with particular reference to charge sensitive preamplifiers and pulse shaping amplifiers.
Finally, the principles of the pulse height analyzers are described in Section 6.8, and the characteristics of alfa,beta,X,gamma and neutrons spectroscopy are given in Section 7.

2. INTERACTION OF CHARGED PARTICLES WITH MATTER

As said before, charged particles directly ionize as it passes through matter, and the electrons and ions produced are moving in an electron field. In the following are treated separately the interaction with matter of heavy ions, traveling through matter in a straight line, and of electrons, traveling erratically, due to its reduced mass.

2.1 Heavy charged particles

A heavy charged particle loses energy through electrostatic interaction with electrons and nuclei. Interaction with electrons (free or bound) gives rise to excitation or ionization, interaction with nuclei to Rutherford scattering. Only ionization is useful for detecting the particles. The most useful parameter is the "specific ionization" defined as the number of ion pairs produced per unit of path length. Specific ionization is energy dependent.
Specific ionization dE/dx (also called stopping power) is given

by the well known Bethe-Bloch equation:

$$(2.1) \qquad \frac{dE}{dx} = -\frac{4\pi z^2 Z e^4 N}{m v^2} \ln\left(\frac{2mv}{I}\right)$$

where:
z = the atomic number of the incident particle (z=1 for protons and deuterons, z=2 for alpha particles and so on)
Z = the atomic number of the target
e = 1.6 x 10(19) C is the electron charge
m = 9 x 10(-31) Kg is the mass of the electron
N = the number of atoms per m3 of the target; NZ = number of electrons per m3 of the target
v = velocity of the incident particle (m/s)
I = mean ionization potential of the target

Considering that the logarithmic term is slowly changing with energy of incident particle E, it can be written:

$$(2.2) \qquad dE/dx \propto -z^2/E$$

showing the dependence of the specific ionization on atomic number and energy of incident particle.
Introducing the electron density δ_e as the number of electrons per cm^3 of matter, i.e.

$$(2.3) \qquad \delta_e = Z N_A \delta_e / A$$

it can also be written:

$$(2.4) \qquad dE/dx \propto \delta_e$$

showing the dependence of specific ionization on electron density of the target material.
The range of a charged particle can be found by integrating Eq.(2.1) from E_o to zero, where E_o is the initial energy:

$$(2.5) \qquad R = \int_{E_o}^{0} \frac{dE}{dE/dx}$$

and neglecting the logarithmic term:

$$R \simeq E^2 / 8\pi z^2 Ze^4 N \qquad (2.6)$$

In Figures 2.1 and 2.2 are shown stopping power and range of protons, deuterons and alpha particles in Si and Ge.

2.2 Electrons

Interaction of electrons with matter is similar to that of heavy charged particles, with the difference that there is no Rutherford scattering due to the small electron mass, that there is a strong contribution to the stopping power at high energies due to bremsstrahlung radiation, and that multiple effects are frequent, giving rise to an erratic pathlength of the electrons. For that reason it is preferable to use, in the case of electrons, the zero transmission range, as the thickness of material absorbing 100% of incident electrons. In Figure 2.3 is shown the range of electrons versus energy for Ge and Si, which are typical detector materials, and if Figure 2.4 is shown the range of electrons in water. The ranges were obtained in the "continuous- slowing-down approximation", in which electrons are assumed to lose energy continuously along their track, with a mean energy loss per unit pathlength given by the stopping power.

3. INTERACTION OF X AND GAMMA RAYS WITH MATTER

Interactions of photons with matter, by which photons are removed or deflected from a primary beam of X or gamma radiation, may be classified according to:

-the kind of target, e.g. electrons, atoms or nuclei with which the photon interacts, and

-the type of event, e.g. scattering, absorption, pair production etc. which takes place.

Possible interactions are summarized in Table 3.1. From a quantitative point of view, the most important interactions are:

1. the photoelectric effect
2. the Compton scattering
3. the Rayleigh scattering and
4. the electron-positron pair production.

TABLE 3.1 - Classification of elementary photon interactions

Type of interaction	Absorption	Scattering	
		Elastic	Inelastic
Interaction with			
atomic electrons	photoelectric effect (bound elec)	Rayleigh scattering	Compton scattering
	(low energy)	(low energy)	
	(high energy)		
nucleons	photonuclear reactions	nuclear scattering	nuclear scattering
Electric field	electron-positron pair production	Delbruck scattering	

3.1 The photoelectric effect

In the atomic photoeffect, a photon disappears and an electron is ejected from the inner shell of an atom. The electron carries away all the energy of the photon, minus the energy binding the electron to the atom. After the electron is removed from a inner atomic shell (K,L,M...) an X-ray or an Auger electron are emitted, the alternative depending on the fluorescence yield. From the conservation of the energy:

$$E_{el} = E_{o} - E_{B} \qquad (3.1)$$

where:
E_{o} = the energy of the incident photon
E_{el} = the kinetic energy of the ejected electron
E_{B} = the binding energy of the electron.

If the photon energy drops below the binding energy of a given shell, an electron from that shell cannot be ejected. Hence, a plot of photoelectric cross section (proportional to the photoelectric effect probability) versus photon energy exhibits the characteristics "absorption edges". Photoelectric interactions are most probable when the photon energy is only slightly more than the binding energy.
After the electron is ejected, the irradiated atoms emit X-rays

resulting from the decay of the excited states. Each element emit a characteristic set of X-rays. A sample containing several elements will therefore emit many X-rays of characteristic energies. The photoelectric effect is also the basis for the X-ray fluorescence (XRF) analysis.
The cross section for photoelectric effect is proportional to the atomic number Z of the sample as:

Z^4 in the low energy region
Z^5 in the high energy region

3.2 The Compton scattering
In Compton scattering, a photon collides with an electron, loses some of its energy and is deflected from its original direction. Considering an incident photon of energy E_0 , the Compton effect gives rise to an electron of energy E_e and a secondary photon of energy E_c ,scattered through an angle ϑ with respect to its original direction.
The basic theory of this effect, assuming the electron to be initially free and at rest, is that of Klein and Nishina. Departures from it occur at low energies because of electron binding effects.
The relation between photon deflection and energy loss for Compton scattering is determined from conservation of momemtum and energy between the photon and the recoiling electron. This relation can be expressed as:

(3.2) $$E_c = \frac{E_0}{1 + \alpha(1 - \cos\vartheta)}$$

where:
$\alpha = E_0/m_0c^2$ is the reduced energy of the incident photons and $m_0c^2 = 511$ keV is the rest mass energy of the electron.
Energy of Compton scattered photons versus scattering angle, for $E_0 = 32$ and 60 keV are shown in Figure 3.1.
The scattering angle can take on values anywhere between 0 and 360 degrees. The angular distribution for the Compton scattered X or gamma rays can be calculated with the Klein-Nishina formula, modified for electron binding effects.
The binding corrections have usually been treated in the impulse approximation, taking into account not only the K-shell, but all the atomic electrons. This involves applying a multiplicative correction, the so-called "incoherent scattering function" S(q,Z) to the differential Klein-Nishina formula:

(3.3) $$\frac{d\sigma(\vartheta)}{d\Omega} = S(q,Z)\,\frac{d\sigma_{KN}(\vartheta)}{d\Omega}$$

where:
$d\sigma_{KN}(\vartheta)/d\Omega$ is the Klein-Nishina differential cross-section and S(q,Z) represents the incoherent scattering function where $q = \sin\vartheta/2\,/\,\lambda$ is the momentum transfer and $\lambda = 12398/E(eV)$.
The Klein Nishina differential cross-section is given by:

(3.4) $$\frac{d\sigma_{KN}(\vartheta)}{d\Omega} = \frac{r_0^2}{2}\left[\frac{1}{[1+\alpha(1-\cos\vartheta)]^2}\left[1+\cos^2\vartheta+\frac{\alpha^2(1-\cos\vartheta)^2}{1+\alpha(1-\cos\vartheta)}\right]\right] \frac{cm^2/el}{sterad}$$

By integrating Eq. (3.4) over all angles the total K-N cross section is obtained, which for low photon energies ($\alpha \ll 1$) may be expressed as:

(3.5) $$\sigma_{KN} = \frac{8}{3}\pi r_0^2 \frac{1}{(1+2\alpha)^3}\left(1+\alpha+\frac{9}{5}\alpha^2+\frac{3}{2}\alpha^3+\ldots\right) \quad cm^2/el$$

In the low energy limit $\alpha \longrightarrow 0$, the total Klein-Nishina cross section becames the classical Thompson cross section:

$$\sigma_T^{el} = \frac{8}{3}\pi r_0^3 = 0.665 \text{ barn/electron}$$

and

(3.6) $$\sigma_T^{at} = \frac{8}{3}\pi r_0^3 Z = 0.665 \text{ barn/atom}$$

The incoherent scattering function S(q,Z) versus momentum q for

Z = 7.5 (water) is shown in Figure 3.2.
The differential cross section for Compton scattering in water at 20 and 40 keV is shown in Figures 3.3 and 3.4.

3.3 Rayleigh scattering

Rayleigh scattering is a process by which photons are scattered by bound atomic electrons and in which the atom is neither ionized nor excited. The scattering from different parts of the atomic charge is then "coherent" i.e. there are interference effects.
This process occurs mostly at low energies and for high Z materials, in the same region where electron binding effects influence the Compton effect. Indeed, if each atomic electron contributes independently to the cross section, the onset for Rayleigh scattering for low momemtum transfer would exactly compensate for the reduction of Compton scattering due to binding.
In practice, by calculating Rayleigh scattering, it is necessary to consider the charge distribution of all Z electrons at once, which can be done approximately through use of an "atomic form factor" F(q,Z). The square of F is the probability that the Z electrons of an atom take up a recoil momentum q, without absorbing any energy. Figure 3.5 shows the atomic form factor versus momentum transfer for water.
The differential cross section for Rayleigh scattering, extended over the Z electrons of an atom is given by:

(3.7) $$\frac{d\sigma_R}{d\Omega} = \frac{r_0^2}{2}(1+\cos^2\vartheta)\left[F(q,Z)\right]^2 \quad (cm^2/\text{atom})/\text{sterad}$$

Integrated angular distributions of Rayleigh cross section gives rise to a probability which is small respect to photoelectric and Compton effects. The differential cross section for coherent scattering in water, at E_0 = 20 and 40 keV, is shown in Figures 3.3 and 3.4.

Rayleigh scattering can be of importance in interpretating "narrow beam" attenuation because of its angular spread.
A useful simple criterion for judging the angular spread of Rayleigh scattering is:

(3.8) $$\vartheta_c = 2 \arcsin\left(\frac{0.0133\, Z^{1/3}}{E}\right)$$

where ϑ_c is the opening half angle of a cone containing at least 75% of the Rayleigh scattered photons.

3.4 Electron-positron pair production
In this effect, which is the most common at high energies ($E \gg$ 1 MeV), a photon disappears in the field of a charged particle, and an electron-positron pair appears.
The cross section for pair production in the field of a nucleus varies as:

(3.9) $$\sigma_p \propto Z^2$$

3.5 Attenuation of X and gamma rays in matter
When a narrow beam of monoenergetic photons with energy E_o and incident photon flux intensity N_o (photon/unit time and area) passes throughan homogeneous absorber of thickness x(in cm), then the emerging photon intensity will be given by:

(3.10) $$N = N_o e^{-\mu x}$$

where:
$\mu(\rho, Z, E)$(in cm^{-1}) is the linear attenuation coefficient for material of physical density ρ (g/cm^3) and atomic number Z.
The attenuation coefficient can be decomposed into contributions from each above described mode of photon interaction as:

(3.11) $$\mu_t = \mu_{ph} + \mu_c + \mu_R + \mu_p$$

where $\mu_{ph}, \mu_c, \mu_R, \mu_p$ designate photoelectric effect, Compton scattering, Rayleigh scattering and pair production respectively. As observed in the Section 1, the detection of ionizing radiation is based on the occurrence of interaction into the detector. This condition corresponds to $\mu_t \neq 0$ and therefore $N < N_o$; the ratio $\varepsilon = (N_o - N)/N_o$ corresponding to the percentage of photons interacting with the matter of the detector is called "intrinsic efficiency" of the detector and is a function of energy of incident photons. Total linear attenuation coefficients of Si and Ge are shown in Figures 3.6 and 3.7.

4. INTERACTION OF NEUTRONS WITH MATTER
Neutrons are not directly ionizing, but are interacting in various manners with the matter, producing (or accelerating) charged particles as secondary products, which then ionize the matter.
The following three types of reactions are the more common for the neutrons:
a) elastic scattering with a nucleus

b) inelastic nuclear reactions
c) nuclear fission.

In all these reactions, in which there is a loss of energy from the neutron to a charged particle, or production of a charged particle, there is finally ionization of the matter.
a) elastic scattering neutron-nucleus
The energy ΔE E loss from the neutron and due to an elastic neutron-nucleus scattering, is given by:

$$\Delta E = \frac{4 M m}{(M+m)^2} E_0 \cos^2 \vartheta \qquad (4.1)$$

where:
m = mass of the neutron
M = mass of the nucleus
E_0 = the energy of the incident neutron and
ϑ = the angle between initial and final direction of the neutron.
In the case of a central collision, ΔE is maximum, i.e.:

$$\Delta E_{max} = \frac{4 M m}{(M+m)^2} E_0 \qquad (4.2)$$

When M = m (collision of a neutron with a hydrogen nucleus), then $\Delta E_{max} = E_0$; the maximum loss of energy is therefore related to a centralcollision neutron-hydrogen, in which the neutron transfers its total energy E_0 to the atom of hydrogen.

b) Nuclear reactions
Among the inelastic nuclear reactions, we have to consider as important those giving rise to charged particles with a high cross sections. In particular the following, listed in Table 4.1:

Table 4.1 - Useful reactions for detection of neutrons

Li^6	+ n	⟶	H^3 + α	+ 4.76 MeV
Li^6	+ n	⟶	H^4 + d + n	- 1.53 MeV
Li^6	+ n	⟶	He^6 + p	- 2.75 MeV
B^{10}	+ n	⟶	Li^6 + α	+ 2.78 MeV
He^3	+ n	⟶	H^3 + p	+ 765 keV
Li^6	+ n	⟶	H^3 + α	+ 4.78 MeV

The reaction $B^{10}(n,\alpha)\ Li^6$ is mainly used for thermal neutrons, and the cross section for the process is inversely proportional to the neutron velocity, in the interval from 0 to about 30 keV (Figure 4.1).
For that reason the sensitivity of detectors employing B^{10} is very low for rapid neutrons. A B-detector for rapid neutron can be obtained by employing also a moderator in addition to the B^{10}.
For neutrons having energy higher than hundreds of keV the last two reactions of Table 4.1 may be usefully employed

c) Nuclear fission

Heavy nucleus bombarded with neutrons fission, in general, into two parts, with a big production of energy in form of kinetic energy of the fission products:

$$K \rightarrow K_1 + K_2 + \quad 200 \text{ MeV}$$

For the detection of thermal neutrons, isotopes like U^{238} and Pu^{232} are employed, and for the detection of epithermal and rapid neutrons, the following threshold reactions can be employed, listed in Table 4.2:

Table 4.2 - Threshold reactions for detection of rapid neutrons

Material	Threshold (MeV)
Pu^{232}	0.5
Np^{237}	0.75
U^{238}	1.45
Th^{232}	1.75
Bi^{209}	5.0

5. DETECTORS

5.1 Introduction and physical principles

As pointed out in Section 1, detectors for charged particles, neutrons and X-or gamma rays are based on the direct or indirect production of secondary charged particles in the detector volume, on the ionization of the detector material and finally on the collection of the electrons and ions by an electric field.
Considering a detector filled with gas (a ionization chamber or a proportional gas-counter filled with Kr at 1 atm.) and an incident photon, for example a X-ray of energy E_o = 20 keV, the different phases of the detection process are the following:
a) interaction of the photon with the gas, through for example a photoelectric effect, which is the most probable at that energy; an electron with energy (E_o - E_b) is then produced, which has a range of micrometers in the gas;
b) ionization of the electron as it passes through the gas; assuming an average ionization potential in Kr of 30 eV, about 700 pairs electron-ions are produced;
c) by polarizing the two plates of the ionization chamber or the anode of the proportional gas counter, the electrons are moving toward the anode, and the ions toward the cathode; considering

that the mass of the ion is about 1800 x 36 times the mass of the electron, the acceleration given to the electron is also much higher than that of the ion, and therefore the collection time will be much shorter for the electron.

a) at incident energies E_o = 20 keV, the photoelectric effect, in the gas Kr at 1 atm, is largely prevailing (about 100 times more than coherent and incoherent scattering). The total mass attenuation coefficient is about 82 cm^2/g and the density of Kr 0.0037; the linear attenuation coefficient is therefore 0.3 cm^{-1}, and for a detector of 5 cm lenght, Eq. (3.10) gives rise to:

$$N = N_o \exp(-5 \times 0.3) = N_o\, 0.22$$

the probability that a photon of 20 keV interact inside the detector is therefore 78%, and 22% is the probability of photoelectric effect in the first cm, 20, 14, 10, and 8 in the successive respectively, according to the exponential law.
Following the photoelectric effect in Kr in the K-orbit (K-edge 14.3 keV) an electron of 5.7 keV is produced, which has a range of micrometers in the gas of the detector.
b) in the hypothesis that the X-rays produced in the gas escape from the detector, the 5.7 keV electron ionizes the Kr-gas atoms; about 200 electron-ion pairs are produced along the electron pathway, corresponding to an electron charge of q = - 3.2 x 10 C;
in the hypothesis that the X-rays produced in the gas (mainly X_K and X_L -rays) interact with the gas atoms, again by photoelectric effect, a larger number of pairs will be produced, corresponding to a larger charge;

c) in the presence of an electric field, electrons and ions are accelerated, following the relationship:

$$a = (e/m)\, E$$

electrons are subjected to an acceleration about 2000 A times larger than the ions (where A is the atomic mass of the ion) due to the reduced mass.
Assuming a ionization chamber with a potential difference of 5000 V between the plates, at a distance of 5 cm, the acceleration of the electron will be: a = 1.8 x 10^6 m/s , giving rise to a collecting time for the electrons (in void) of about 25 ns.
During migration of charges between cathode and anode a current will be generated, composed by electron current $I_-(t)$ and ion current $I_+(t)$. When n_- and n_+ are the charges and t_- and t_+ the migration times, and d the distance between the electrodes, then:

(5.1) $$I(t) = (n_- e)/t_- + (n_+ e)/t_+$$

where t = d/v.

5.2 Gas-filled detectors

A gas-filled detector is basically a metal chamber filled with gas which contains a positive anode wire. A charged particle or ionizing radiation passing through the gas produces free electrons and positive ions by the interaction processes described above. The electrons are attracted to the anode and collected to produce an electric pulse.

At low anode voltages the electrons produced may recombine with the ions and the signal is reduced. At a sufficient high valtage nearly all electrons are collected, and the detector is known as a ionization chamber. At higher voltages the electrons are accelerated toward the anode at energies high enough to ionize other atoms, thus creating a larger number of electrons. Over a wide voltage range the output pulses, which are now much larger than for an ionization chamber, are proportional to the original ionization, and therefore to the energy of the incident particle. At higher voltages the electron multiplication is greater yet, and the number of electrons collected is independent of the inizial ionization. The region is that of the Geiger-Muller counter, where the large output pulses are the same for all incident radiation or particles.

The most common gases for charged particles and photons are high purity neon, argon, krypton and xenon.

The different voltage regions are shown schematically in Figure 5.1.

a) Charges in an electric field

We have previously discussed that when a charged particle or a X- or gamma photon interact with the gas of a detector, electrons and ions are produced. Electrons are attracted to the anode and, depending on the electric field, may ionize other atoms creating new electrons and so on. The increasing of electrons per unit pathway may be described through the "Townsend coefficient"

α E/p (E is the electric field and p the gas pressure). If the electric field is homogeneous, and we have n electrons at position x (see Figure 5.2), the increasing of electrons in the pathway dx will be given by:

$$dn = n \, \alpha dx \tag{5.2}$$

and if n_o is the number of electrons at the cathode, the final number of electrons at the anode will be given by:

$$n = n_o \exp \int_0^d (\alpha dx) \tag{5.3}$$

During the movement of electrons from cathode to anode, and of ions from anode to cathode, a current will be generated given by Eq. (5.1) i.e.:

(5.4) $$I(t) = n_- e/t_- + n_+ e/t_+$$

the electronic current will be thousends of times larger, due to the shorter collection times, but will also lasts thousends of times less (Figure 5.3).
The detector may be approximated as a capacitor into which a
charge is deposited. During the charge collection a small current flows, and the voltage drops across the bias resistor. The schematic set-up of the detector is shown in Figure 5.4.
The pulse voltage across the bias resistor R may be calculated, using the Kirchhoff rule:

(5.5) $$C\, dV/dt + I(t) = V(t)/R$$

The solution of this differential Equation is given by:

(5.6) $$V(t) = 1/C \exp(-t/RC) \int_0^t \exp(t/RC) I(t) dt$$

and considering Eqs (5.4):

(5.7) $$V(t) = \frac{n_o e}{C}\left\{\frac{1}{t_-} - \frac{1}{t_+}\right\} \frac{1}{\alpha v_- + \frac{1}{RC}} \left\{\exp(\alpha v_- t) - \exp(-t/RC)\right\}$$

This Equation can be characterized through three time constants:

$\tau = RC$
$\tau_- = 1/\alpha v_-$
$\tau_+ = 1/\alpha v_+$.

The most interesting approximation occurs when:

(5.8) $\tau > \tau_+$ i.e. $RC \gg 1/\alpha v_+$

In this case following Equations may be deduced:

$$V(t) \cong (e\, n_o)/Cd \exp(\alpha v_- t) \qquad 0 \ll t \ll t_-$$

(5.9) $$V(t) \cong (e\, n_o)/Ct_- \exp(\alpha d\, t) \qquad t_- < t < t_+$$

$$V(t) \cong \exp(-t/RC) \qquad t > t_+$$

Equations (5.9) are depicted in Figure (5.5)
When:

(5.10) $t \gg t_-$ i.e. $RC \gg 1/\alpha v_-$

then $\exp(t/RC) \gg I(t)$ and therefore:

(5.11) $$V(t) \cong R\, I(t)$$

and the curve of pulses (Figure 5.6) is proportional to the current curve (cfr. Fig. 5.3).

b) Ionization chamber
The very low signal output for the ionization chamber makes this detector difficult to use for detecting individual photons or particles. For that reasons, itfinds more use in high radiation fluxes in which the total current produced can be very large.
A typical ionization chamber is shown in Figure 5.7.
Ionization chambers for charged particles and photons are filled with gases like argon,krypton, xenon,neon plus 5-10% CO_2 or CH_4.
For detection of neutrons, ionization chambers are filled with B, generally enriched in B^{10}, for detection of thermal neutrons. Boron is used or in the form of gas (BF_3) or the electrodes are covered with a thin B-sheet.
Very used are also ionization chambers using fission reactions. In this case the chambers are filled with a gas containing one of the material listed in Table 3.3 or the electrodes are covered with fissionable materials.
Also ionization chambers may be used with the detector filled with a gas like hydrogen, giving rise to backscattered protons when interacting with neutrons.
Many radiation monitoring instruments use ionization chambers.
In the case of ionization chamber, the pulse is proportional to the energy of incident particle, and for particles of different energies, an energy "spectrum" can be determined (see also Spectroscopy).
In the case of the ionization chamber, the Townsend coefficient is zero because there is no multiplication of electrons in the detector. The current is therefore given by Eq. (5.3) and the pulse function V(t) can be calculated from Eq. (5.7):

(5.12) $$V(t) = (n_o e)/C\,(1/t_- + 1/t_+)\,RC\,(1-\exp(-t/RC))$$

If the time constant RC is large compared to the collecting times for electrons and ions, then: $\exp(-t/RC) \cong 1 - t/RC$, and Eq.(5.12) may be written as:

(5.13) $$V(t) = ((n_o e)/Ct_-)t + ((n_o e)/Ct_+)\,t$$

The electrons are first drifting to the anode in the time interval 0 - t_-, giving rise to the pulse $V_-(t)$; in the meantime the ions were almost at rest; they drift in the time interval

$t_- \leq t \leq t_+$, giving rise to the pulse $V_+(t)$. The electron and

ion pulses, shown in Figure (5.7) increases linearly with the time, following Eq.(5.13).
When, at the contrary, RC is selected larger than t_- but smaller than t_+, then Eq. (5.12) may be written as:

(5.14) $$V(t) = \left(\frac{n_o e}{C t_-}\right) t + \left(\frac{n_o e}{t_+}\right) R \left(1 - e^{-t/RC}\right)$$

The pulse versus time is shown in Figure (5.8).

c) The proportional counter
A proportional gas counter consists of a metallic container, generally cylindrical (cathode) with a thin electrode (anode) in the center carrying a positive bias voltage. The container is filled with a special gas mixture (noble gas + methane). An example of cylindrical gas proportional counter is given in Figure 5.9.
Many different gases are used, depending upon the range of particle or X-ray energies of interest. For very low X-ray energies, around a few keV, a mixture of He and methane is used. Higher energies require Ne,A,Kr or Xe, utilizing the greater probability of a photoelectric effect as the atomic number of the absorbing gas is increased.
When used for detecting neutrons, a proportional counter is filled with BF_3 (thermal neutrons), He or Li for epithermal neutrons, with a gas containing one of the materials listed in Table 3.3 for rapid neutrons. In alternative, the anode may be covered with elements or isotopes like B^{10}, Li^6, U^{238}, Pu^{232} or others, according to the energy to be detected.
The operating voltage of a proportional counter depends upon the gas mixture and the geometry. At too low voltages, the electrons may not accelerate sufficiently to ionize other molecules (ionization chamber region), where at too high voltages the electrons may ionize virtually all atoms producing a pulse independent from the initial photon energy (Geiger-Müller region). Between the two above cited region, and over a wide voltage range (between about 1500 and 2500 Volts) the output pulse is proportional to the energy of incident X-ray.
The electric field inside a cylindrical gas proportional counter is not homogeneous, and is given by the Equation:

(5.15) $$E = V_o / \log (r_a / r_i) \; (1/r)$$

where:
V_o = the operating voltage between anode and cathode
r_a = the radius of the cylindrical container
r_i = the radius of the wire constituting the anode.

The electrical field is therefore strongly increasing in asmall region close to the anode (multiplication region). In this region an electron accelerates toward the anode at energies high enough to ionize other atoms.

Assuming n_o electrons are produced by primary ionization in the gas, the final number of electrons will be given by Eq. (5.3). If γ is the probability that an electron produces a second photoelectron, then n electrons will generate γn after the first avalanche, $(\gamma n)n$ after the second avalanche and so on, giving rise to the serie:

(5.16) $$n_t = n + \gamma n^2 + \gamma^2 n^3 + \ldots.$$

for proportional gas counters, it should be $(\gamma n) << 1$, and Eq.(5.16) can be written as:

(5.17) $$n_t = n/(1-\gamma n) \cong n_o \exp \int \alpha \, dx$$

From Eq. (5.15) the pulse may be calculated, which is:

(5.18) $$\Delta V = \frac{n_t e}{C \ln\left(\frac{r_a}{r_i}\right)} \ln \frac{r}{r_o}$$

showing its proportionality to the primary electrons n_o .

d) Geiger-Müller counter
The Geiger-Muller counter can be considered like a proportional gas counter working at higher voltages (3000 Volts or more).
The Geiger-Muller counter produces a large voltage pulse that is easily counted without any further amplification. No energy measurements are possible since the output pulse height is independent of initial ionization. G-M counters are available in a wide variety of sizes, generally with a thin mica window. The operating voltage is in the plateau region (see Figure 5.1). which can be very flat for a few hundreds volts. The plateau is determined by measuring the counting rate as a function of the anode voltage.
The discharge produced by an ionization must be quenched in order for the detector to be returned to the initial state for the next pulse. This is accomplished by using a fill gas that contains a small amount of halogen in addition to a noble gas. The voltage drop across a large resistor between the anode and bias supply will also serve to quench the discharge since the operating voltage will be reduced below the plateau.
The G-M counter is inactive after each pulse until the quenching is complete. The dead time is of the order of hundreds of microseconds long, which limits the counter for high count applications.

5.3 Scintillation detectors

There are compounds or mixtures or elements producing a pulse of light when irradiated with charged particles (primary or secondary).
These materials are called scintillators and can be used as detectors for charged particles or for ionizing radiation.
The light pulse produced is very small, and is amplified and converted to an electric pulse by a "photomultiplier tube". The photomultiplier consists of a photocathode, a focusing electrode (anode) and 10 or more dynodes that multiply the number of electrons striking them several times at each dynode. The anode

and dynodes are biased by a chain of resistors typically located in a plug-in tube base assembly (Figure 5.10).
There are various classes of scintillators:
-inorganic scintillators
-organic scintillators
-gas scintillators

5.3.1 inorganic scintillators

The properties of a scintillation material required for good detectors are transparency, availability in large size and large light output proportional to incident radiation. Relatively few materials have good properties for detectors. Thallium activated NaI and CsI are commonly used, as well as a wide variety of plastics. In recent times and for CT-scanners, also BGO and CsF crystals are used.
The light is emitted from a scintillator with an exponential law of the type:

$$L(t) = L_0 \exp(-t/\tau_{fl.}) \quad (5.19)$$

where $\tau_{fl.}$ represents che fluorescence constant of the process, which is depending on the type of ionizing particle.
The most important characteristics of the most common scintillators, inorganic and organic (wavelenght oftheemission, scintillation efficiency, fluorescence constant) are shown in
Table 5.1.

Table 5.1 - Characteristics of the most common scintillators

Scintillator material	wavelenght at maximum emission (nm)	decay constant (ns)	sc.convers. efficiency (%)	density (g/cm³)
NaI(Tl)	415	230	100	3.67
CsI(Tl)	565	1000	45	4.51
CsI(Na)	420	630	85	4.51
CsF	390	5	5	4.64
CdWO	540	5000	40	7.90
CaF (Eu)	435	630	50	3.19
Bi Ge O	480	300	12	7.13
ZnWO	480	5000	26	7.87
Li I(Eu)	480	1400	35	4.08

Attenuation coefficients of NaI, CsI, BGO, CaF_2 and BaF_2 are shown in Figures 5.11 to 5.15.
Concerning medical applications, two scintillation detectors have been identified as possessing properties superior to NaI(Tl) for CT scanners: the first to be tried was calcium fluoride doped with Europium: CaF_2(Eu).
This detector is made of a transparent, hard material useful for detecting X and gamma rays up to several hundred keV. This crystal is less efficient than NaI, but has the notable characteristics of the lack of long term light decay following

intense excitation, like in tomography. The dacay constant of CaF(Eu) is 0.94 μs.
A second scintillator that is adopted widely in CT is bismuth germanate (usually called BGO). This crystal has attractive properties. It has a high attenuation coefficient, due to its high atomic number and density, and therefore provides an efficiency of almost 100% for X-rays employed in CT-scanners. Further is has a short decay constant of about 0.3 μs, and a very low afterglow.

5.3.2 organic scintillators
Many organic materials can be employed as scintillators. Among them we may remember benzene (C_6H_6), Xylene ($C_6H_4(CH_3)_2$), naphtalene ($C_{10}H_8$) ,anthracene ($C_{14}H_{10}$) and plastics.The last are the most important.
Many types of plastic scintillators are now comercially available, and find application in fast timing, charged particles or neutron detection, or in cases where very large sizes are appropriate. The active component is usually anthracene, mixed in various amounts in a polyvinyl toluene base. Sub nanosecond rise times are achieved with plastic detectors coupled to fast photomultipliers, and these assemblies are ideal for fast timing work.
The energy resolution of plastic scintillators for X-rays is very poor compared to NaI and the efficiency of organic materials for gamma absorption is low (all low Z elements).
Organic scintillators can be also used for detection of neutrons, especially of high energy, because of the high content of hydrogen, giving rise to high energetic protons.
Also scintillators with addition of B^{10} or Li^6 can be used for detection of neutrons, following the mechanisms discussed in Section 4.
5.3.3 Inorganic scintillator and photomultiplier
In Figure 5.10 it has been shown a schematic set-up of a typical inorganic scintillator (for example a NaI) with photomultiplier. The system is working as a detector in the following manner:
a photon (X-ray or gamma ray) enters in the detector and interacts with the detector material according to the four processes examined in Section 3, producing one or more electron. The

electrons will ionize as they passes through matter. The scintillators have the property of emitting light when ionized. The light will be directed to the photocathode, where the light is converted in electrons.
The electric field between photocathode , dynodes and anode accelerate the electrons to the first dynode, in which they arrive with enough energy to "extract" more electrons, which are all accelerated to the second dynode where they extract again more electrons and so on. Finally, a large number of electrons will reach the anode giving rise to a current and therefore to a pulse along the bias resistor.
The anodic current is depending on the fluorescence constant and on the transit time t of the electrons in the photomultiplier

(see Figure 5.16). Further, for a constant transit time, the current is a function of the type of incident particle (Figure 5.17).

5.4 Semiconductor detectors

5.4.1 the physical process

A solid can be schematized as constituted by single atoms interacting reciprocally by means of their electric and magnetic fields, which contribute to separate in bands the electronicle-vels.In the extreme case of an insulant, the two lowest bands, the valency band and the conduction band are completely separated with a bandgap of about 5 eV (Fig.5.18). For example in a diamond crystal,all electrons are in the valence band and are not able to move. The conduction band is void and cannot be reached by valency electrons following only thermal collisions. The passage of a particle or a photon of sufficient energy could move the electron to the conduction band, generating a current.

On the other side, in the case of conductors, there is an overlap between the two bands, and a continuous passage of electrons (Fig. 5.18).

The case of semiconductors is intermediate, in the sense that there is a bandgap between valency and conduction band, but the energy gap is reduced and also at room temperature there are electrons migrating from the valency to the conduction band. At low temperatures, a semiconductor works like an insulator. At high temperature a conductivity is strongly increasing. When a thermal collision excites an electron to the upper band, a positive ion remains in the lower level. An external electric field moves therefore electrons and ions like in a ionization chamber. In fact the ions are not really moving but is moving the positive "vacancy".

Pure germanium is called an "intrinsic semiconductor" and is employed as a detector at liquid nitrogen temperature.

A small amount of conduction electrons in Ge or Si may modify its properties. For example, adding traces of As pentavalent to Ge tetravalent will increase the conductivity of the crystal, because only 4 As electrons can be used to bind Ge, and the fifth will be free to drift to the conduction band, with only a small amount of energy. Ge with traces of As or of a pentavalent element is called semiconductor of the n-type.

At the contrary a trivalent trace element will give rise to a hole conduction, like for example in the case of B. Ge with traces of B or of a trivalent element is called semiconductor of the p-type.

A junction of the type p-n acts like a diode. The current versus voltage of a p-n junction is shown in Figure 5.19.

Also other materials besides Ge and Si may be used as semi-conductor detectors, like As, Cd, Te, Hg.

An inverse p-n junction, used as a detector, is constituted by a thin window of a n semiconductor and a p semiconductor of adequate thickness (Figure 5.20). The distribution ofcharges, the current and thevoltage inside the semiconductors, are also shown in Figure 5.20.

It may be observed that the pulse versus time is similar to that of a ionization chamber.

5.4.2. Energy necessary to create an electron-hole pair

The energy lost by charged particles or ionizing radiation in semiconductor detectors ultimately results in the creation of

electron-hole pairs. The average energy $\bar{w}$ necessary to create a pair in a given semiconductor at a given temperature is independent of the type and the energy of the ionizing radiation. The values for Si and Ge are: 3.62 eV in Si at room temperature; 3.72 eV in Si at 80 K, and 2.95 eV in Ge at 80 K.
Since the forbidden bandgap value is 1.115 eV for Si at room temperature and 0.73 eV for Ge at 80 K, it is clear that not all the energy of the ionizing radiation is spent in breaking covalent bonds. Some of it is released to the lattice in form of phonons.

5.4.3 Characteristics of semiconductor detectors
The Table 5.2 gives some of the most important characteristics of various semiconductors as detector materials, i.e. mean atomic number, bandgap, energy necessary to create an electro-hole pair and Fano factor. This last will be discussed in Section 12.

Table 5.2 - Characteristics of various semiconductors

Material	Z	Bandgap (eV)	Energy/e-h pair (eV)	Fano factor
Si	14	1.12	3.61	0.1
Ge	32	0.74	2.98	0.1
CdTe	48-52	1.47	4.43	7
HgI	80-53	2.13	4.2	0.27
GaAs	31-33	1.43	4.2	0.18

Concerning the attenuation of X-rays in semiconductors, for example 10 keV X - rays have a mean penetration of 12 μm in HgI, 15 μm in CdTe, 55 μm in Ge and 120 μm in Si, while 100 keV photons have a mean penetration of 0.5, 1.1, 5 and 115 mm respectively. At present the largely most used semiconductor detectors are Ge and Si. As a practical matter both Ge and Si photon detectors must be cooled in order to reduce the thermal charge carrier generation (noise) to an acceptable level. The common medium for detector cooling is liquid nitrogen. The detector element and in

general also the preamplifier are housed in a clean vacuum chamber which is attached to a Dewar. The detector is in thermal contact with the liquid nitrogen which cools it around 77 K. At these temperatures, reverse leakage currents are in the range of 10(-9) to 10(-12) A. A cross sectional view of a typical cryostat is shown in Figure 5.21.

5.4.4 Si-charged particle (surface barrier) detectors
Silicon charged particle detectors have a p-i-n structure in which a depletion region is formed by applying bias, with the resultant electric field collecting the electron-hole pairs produced by an incident charged particle. Detectors are generally available with depletion depths of 100 to 1000 μm, with the cost proportional to the depletion depth. Detectors are specified in terms of surface area and alpha or beta particle resolution as well as depletion depth. The resolution depends slightly upon detector size, being best for small area, thin detectors. Alpha resolution of 15 to 35 keV and beta resolutions of 7 to 30 keV are typical. A chart of energies of various particles that can be measured with 100 to 1000 micron depletion depth is shown in Table 5.3.

Table 5.3 - Maximum particle energy versus Si-depletion depth

Depletion depth (μm)	Maximum particle energy (MeV)		
	Electron	Proton	Alpha
100	0.15	7	15
300	0.31	15	55
500	0.45	21	85
700	0.52	27	105
1000	0.73	33	130

5.4.5 Photon detectors
a. X-ray detectors
The optimum high resolution detector for photon energies from 1 to about 30 keV is the planar Si(Li) detector, which specifications are given in terms of active diameter (mm) and energy resolution at 5.9 keV (in eV).
Planar Si(Li) detectors have a window thickness of about 0.1 μm, diameter between 4 and 16 mm, and energy resolution of 150-250 eV at 5.9 keV.
From about 3 to about 500 keV, a planar p-type HPGe may beem-ployed, which is characterized by a diameter between 5 and 40 mm, and energy resolution of 160-350 eV at 5.9 keV, and about 500 eV at 122 keV. In the same energy range also a low-energy coaxial detector (LO-AX, n-type HPGe) may be employed, which is characterized by 30-60 mm diameter, and energy resolution of 300-500 eV at 5.9 keV and about 600-700 at 122 keV.
b. gamma-ray detectors

For detection of gamma rays in the energy interval 10 keV -10 MeV

a coaxial HPGe detector of the p-type may be employed, with active volume of 50-120 cm^3 and energy resolution between 1.8 and 2.2 keV at 1.33 MeV.
Special detectors are available for gamma-ray high-count-rate

applications; energy resolution can be mantained constant till about 50000 - 100000 counts/s using selected feedback resistors and acting on the time constant of the main amplifier (see Section 6.6.3).
Also Ge - detectors are available, characterized by a very low background, obtained by a careful materials selection.

Table 5.4 - Typical use of detectors and types of events which can be detected

Ionization chamber:	
	dosimetry
	alpha and beta ray -spectroscopy
proportional gas counter:	
	low energy X-ray spectroscopy (maximum energy depending on the filling gas, minimum energy depending on the window thickness);
	detection of alpha and beta particles
	detection of neutrons (BF_3 -detectors)
Geiger-Muller:	
	dosimetry
	detection of alpha and beta particles
scintillator:	
	high-energy X-ray spectrometry (about 20-100 keV)
	gamma ray spectroscopy
semiconductor-detectors:	
planar Si (thickness: 100 - 500 μm)	

(area 20 -500 mm)	
	alpha and beta spectroscopy
Si(Li)	
(thickness 2-5 mm)	
(area 10-100 mm)	
	X-ray spectroscopy
p-type HPGe-planar	
	X-ray spectroscopy
n-type HPGe-coaxial	
	gamma-ray spectroscopy

5.5 Parameters characterizing a detector
The most important parameters characteriziong a detector are the following:
1. type of particle or photon, which can be detected
2. energy resolution
3. efficiency

1. type of particle or photon which can be detected
In Table 5.4 are collected the detectors related to the types of events which can be detected.

2. energy resolution
The energy resolution of a spectrometer is a measure of its ability to resolve two peaks that are very close together in energy. Observing a typical peak (Figure 5.22), the absolute energy resolution can be defined as the full width of the peak at half of the maximum count level (FWHM), measured in keV, while the relative energy resolution (in %) R is given by:

(5.20) $$R = \Delta E/E_o \times 100$$

where:
ΔE = FWHM (in keV)
E_o = the energy (in keV) at the centroid of the photopeak

The system resolution SR, due tothe detector and to the electronics (preamplifier,amplifierand multi-channel-analyzer) is given by the formula:

(5.21) $$SR = (R_d + R_{el})^{1/2}$$

where:
R_d is the detector resolution
R_{el} is the electronic resolution
These resolutions are said to add in quadrature.
There is a lower limit to R_d which is energy dependent. The charged particles or the secondary electrons produced by the ionizing radiation loses energy in the detector by dE /dx. The average energy required to produce an ionization is depending on the detector material and is about 3 eV in Si and Ge, about 30 in
gases employed for ionization chambers and proportional detectors and about 300 in scintillators.
The production of electron-ion and electron-hole pairs is a

process that is statistical in nature, and hence there are fluctuations in the actual number produced. When the proper statistics are used, the theoretical lower limit to R_d is given by:

(5.22) $$R_d = K (F E)^{1/2}$$

where K is a constant, E is the energy of the photon in keV, and F is the statistical "Fano factor". To a very good approximation for Ge and Si detectors this equation reduces to:

(5.23) $$R_d = 1.44 \sqrt{E} \quad \text{(in keV)}$$

In general the number n of electron-ion or electron-hole pairs are given by:

(5.24) $$n = E / \bar{w}$$

where $\bar{w}$ is the mean energy required for generating a pair. The standard deviation will be given, following the Poisson statistics, by:

(5.25) $$\Delta n = (E / \bar{w})^{1/2}$$

and the relative deviation will be given by:

(5.26) $$R.D. = \Delta n / n = (\bar{w} / E)^{1/2}$$

The intrinsic detector resolution is,therefore, proportional to the square root of the energy needed for creating a pair. For that reason the energy resolution of a semiconductor detector is much better than the resolution of a gas detector or of a scintillator. Exact calculations are more complicated because of the Fano factor.
The energy resolution at various energies for different detector types is illustrated in Table 5.5, and is also shown, versus energy, in Figure 5.23.

Table 5.5 - Energy resolution (in keV) for various detectors at photon energies of 5.9, 122 and 1332 keV

Energy (keV)	5.9	122	1332
prop. counter	1.2	-	-

X-ray NaI(Tl)	3.0	12	-
3x3 NaI(Tl)	-	12	60
Si(Li)	0.16	-	-
Planar Ge	0.18	0.5	-
coaxial Ge	-	0.8	1.8

3. Total detector efficiency

The efficiency of a detector is a measure of how many pulses occur for a given number of incident radiation or particles. Various kinds of efficiency definitions are in common use.

a. absolute efficiency. The ratio of the number of counts produced by the detector to the number of photons or particles produced by the source. This includes the solid angle subtended by the detector, depending upon the source-detector distance.

b. intrinsic efficiency. The ratio of the number of pulses produced in the detector to the number of photons or charged particles striking the detector. This ratio is depending on the stopping power for charged particles, and it is in general 1, when the detector thickness is properly selected. For X-and gamma rays the intrinsic efficiency is depending on the attenuation coefficient of the incident radiation and on the thickness of the detector.

c. Full energy peak (or photopeak) efficiency. The efficiency for producing full-energy peak pulses only, rather than a pulse of any size (for example due to a Compton effect). This efficiency is, of course, 1 for charged particles. For ionizing radiation of energy less than a few MeV, the photopeak efficiency is depending mainly on the ratio ofthe photoelectric effect to the Compton effect for the detector material. For same detector thickness, the photopeak efficiency is larger for higher Z detector material.

6. NUCLEAR ELECTRONICS

6.1 Introduction

As explained in Section 5, when a charged particle oraphoton is detected, a pulse is produced, characterized by a rise time, a decay time, the maximum amplitude and a signal to noise ratio. In order to preserve the maximum signal-to-noise ratio, a preamplifier will in general follow the detector, which is specifically designed to be located close to the detector, and to accept the signal from a detector with minimum shaping. In several cases, when cooled semiconductor detectors are employed, also the preamplifier is cooled. The preamplifier performs also

the function of amplifying the detectro pulses.
After the preamplifier, there is in general an amplifier; amplification is actually the minor role of a nuclear research amplifier. The instrument might best be termed a signal processor, because the major role of an amplifier is to convert the preamplifier output signal into a form most suitable for the measurements desired. In particular,an amplifier is used for shaping,filtering and amplifying the pulses.
Finally, after the amplifier, we have in general a multichannel analyzer, which is the heart of most experimental measurements since it performs the essential functions of collecting the data, providing a visual monitor, and producing output, either final results or raw data for later analysis.
In Figure 6.1 is shown the most simple spectrometry system, composed by a detector, preamplifier, amplifier and multichannel analyzer.

6.2 Detector output and connections to the preamplifier

According to Section 5, a typical pulse from a nuclear detector is characterized by its maximum amplitude (positive or negative),

the rise time, the decay time and the time signal to noise ratio Figure 6.2).
Concerning the amplitude, it is mainly depending on the detector type and on the equivalent circuit of the detector plus preamplifier, i.e. the time at which the pulse is cut-off.
In the case of a semiconductor detector and of a ionizing chamber,
maximum pulses on the order of microvolts to millivolts are obtained; more in particular for an ionization chamber a value of approximately $V = n\ e/C$ can be deduced, where n is the number of pair and C che capacity of the detector.
In the case of proportional detectors, there is an amplification of the number of primary pairs, and the value of the output pulse from the detector is given be Equation (5.18); pulses on the order of millivolts or a little more are obtained.
Finally, in the case of a scintillation detector, the photomultiplier produces a very strons amplification of the electrons, of a factor 10(6) to 10(8). Pulses on the order of volts are therefore obtained, which do not need any further preamplification. The photomultiplier and its characteristics will be discussed in section 6.4.

In the case of the Geiger-Muller detector there is an avalanche effect, and the pulse has a very high amplitude, independent on the energy of the incident particle.
It is again important to note that, except the case of the Geiger-Muller detector, there is a proportionality between energy of incident particle or photon and amplitude of the output pulse.
Concerning the rise time, in the case of a ionizing chamber, it is depending on the collecting time of electrons and ions, and,therefore, on the dimensions of the chamber and on the electric field. To avoid too long collecting times, the pulse due to the ions is cut off, and typical collecting times on the order of tens of microseconds are obtained. In the case of a proportional detector, collecting time are shorter, and typical rise time on the order of microseconds or a little less are achieved.
In the case of semiconductor detectors, the collecting times are extremely short (between ns and ps); for that reason the rise time is depending on the electronics coming after the detector, especially the preamplifier.
In the case of the scintillation detector, the rise time of the pulse at the output of the photomultiplier is mainly depending on the decay constant of the scintillator (see Table 5.1) . For the most common we have decay constants of 0.23 (NaI), 0.63 (CsI) and 0.3 (BGO) microseconds respectively.
Coming to the decay constant of the detector pulse, it is depending on the RC value of the detector equivalent circuit.
In Figure 6.3 is shown the electronic circuit of a nuclear detector, which includes the bias resistor,the total capacity,including the capacity of the detector plus the parallel capacity ofthe cabling between detector and preamplifier and the ground capacity of the system, and the total resistence,which includes the resistence of the detector and the resistences in series of the cabling and parassites.
Through a ionization chamber and a semiconductor detectors there is a passage of current (leakage current), which produces a voltage drop (?) along the bias resistor:

$$V = V_o - R \; i$$

6.3. Different types of preamplifiers

There are basically three types of preamplifiers that are normally used with the describe detectors:
a) voltage sensitive preamplifiers
b) current sensitive preamplifiers
c) charge sensitive preamplifiers

a) The voltage sensitive preamplifier is not widely used for spectroscopy applications since gain is dependent on detector capacitance. On the other hand the detector capacitance does not remain constant when the bias voltage and other parameters change. Therefore the gain instability of the voltage sensitive preamplifier results in unacceptable line broadening for spectroscopy.
b) The current sensitive preamplifier is an amplifying instrument with a relatively low input impedance designed to convert fast current pulses such as those originating at the anode of a photomultiplier to a voltage pulse. The output of the current preamplifier can drive several meters of coaxial cable to deliver the pulse to a fast amplifier with minimum distortion.
c) The charge sensitive preamplifier is preferred for most spectroscopy applications.
The signal from a semiconductor detector or ion chamber is a quantity of charge amounting to a current pulse lasting from 10(-9) to 10(-5) s depending on the type detector and its size.
A typical charge preamplifier coupled with the detector is schematized in Figure 6.4, characterized by a feedback capacitance C_f a feedback resistor R_f and an amplification stage.
For most applications the quantity of charge and/or the time of occurrence of an event are the parameters of interest. A charge sensitive preamplifier can measure both parameters since it integrates the charge on the feedback capacitor; its gain is not sensitive to a change in detector capacitance, and the rise time of the output pulse is equal to the detector current pulse width in the ideal case.
The output voltage from the preamplifier has an amplitude V_o and a decay time constant τ , given respectively by:

(6.1) $$V_o = Q_D / C_f \quad \text{and} \quad \tau = R_f C_f$$

where Q_D is the charge released by the detector, C_f is the feedback capacitor (0.1 to 5 pF) and R_f is the feedback resistor. R is a noise source and is made as large as possible consistent with the signal energy - rate product and the detector leakage current in the direct coupled system.
6.4 characteristics of the charge-sensitive preamplifier
The preamplifier is kept small to permit mounting it as close as possible to the detector, thus reducing input capacitance causing by cabling and decreasing microphonic noise, ground loops, and radio frequency pickup, all of which are sources of noise for the charge-sensitive preamplifier.

The "sensitivity" of a preamplifier can be defined, as mV of output pulses per MeV of energy deposited in a given detector material. The charge released by the detector is a function of

the X-or gamma ray or particle energy and the detector material, and is given by:

(6.2) $$Q = (E\ e \times 10^{6})/w$$

where E is the energy in Mev of the incident radiation, e is the charge of an electron, 10^6 converts MeV to eV and w is the amount of energy required to produce an electron-ion or an electron -hole pair in the detector.
From Eqs. (6.1) and (6.2) and for C_f = 1 pF, the maximum amplitude of the pulse at the output of the preamplifier will be:

$$V = E \times 10 \times 1.6 \times 10 / 10 \times 3.7$$
$$= 0.043\ E(MeV) \quad volts = 43\ mV/MeV$$

for example for 100 keV photons V = 0.43 mV.
The preamplifier appears as a large capacitor to the detector, equivalent to C A, where A is the gain of the preamplifier. This capacitor must be much greater than the other sources of capacitance on the preamplifier input, such as the detector, input cabling etc. in order for the preamplifier gain to be insensitive to input capacitance gain. Preamplifier gain stability is also depending on the stability of C ,the feedback capacitor, and the preamplifier open loop gain. C should be selected for good temperature stability and the open loop gain is made very large so that small changes on it can be neglected.
Noise in charge-sensitive preamplifiers is generally determined by four components: the input field effect transistor (FET), the total capacitance at the input (C_{in} ,the detector capacitance etc.), the resistence connected to the input, and input leakage current.
The FET is selected for low-noise performance, and in some applications, with semocinductor detectors, it is cooled to liquid nitrogen temperature to improve its performance. In cooled FET applications the detector and preamplifier are generally built as an integral assembly. The preamplifier is designed with minimum internal capacitance. The maior sources of input capacitance are from the detector and from the cabling between the preamplifier and the detector.
Figure (6.5) shows the noise versus external capacitance for a typical preamplifier, measured in terms of energy resolution of a peak.
The noise of a charge-sensitive preamplifier and the capacitance of the detector can be measured by using a calibrated pulser in parallel of a radiation source and detector, and to measure the full width at half maximum with the source with detector,and of the pulser alone, with the pulser peak at same position, in the multichannel analyzer, that with the radiation source.
It is important to observe that, in the case of semiconductor detectors, its sensitive area is important because it affects both sensitivity and energy resolution. In fact detector capacitance and noise are directly proportional to the area, smaller detectors give much better resolution. selecting the right detector size requires a compromise between sensitivity and resolution.
The rise time of the voltage pulse, V ,at the output of the charge sensitive preamplifier in the ideal case is equal to the charge collection time of the detector. When a detector with very

fast collection times or large capacitances are used, the preamplifier itself may limit the rise time of V . A plot of a charge-sensitive-preamplifier output rise time, versus external capacitance is shown in Figure 6.6.
In Table 6.1 are finally shown typical characteristics of commercial preamplifiers, for charged particles with semiconductor detectors, for X-rays with semiconductor detectors and with proportional detectors.

Table 6.1 - Characteristics of typical preamplifiers

detector	sensitivity (mV/MeV)	equivalent input noise (keV at pF)	rise time (ns at pF)	bias resistor (MOhm)
Si(1)	45 mV/MeV	1.6 at 0 3.4 at 100	5 at 0 12 at 100	100
proport.	0.16 V/pair	2.2 at 0	25 at 0	100

In conclusion, the preamplifier output consists of a quasi step function proportional to the input amplitude, which rise time being as fast as the circuit and detector limitations permit, usually less than 50 ns. The step function is followed by a slow exponential decay, usually on the order of 500 microseconds, but varying generally between microseconds and milliseconds, depending on the detector type. A typical sequence of pulses from the preamplifier is shown in Figure 6.7. The preamplifier signal is not suited for being processed, because therelationship between amplitude of the pulse and energy of the incident particle

or radiation is lost.

6.5 Photomultipliers

The photomultiplier tube or phototube is an integral part of a scintillation counter. Without the amplification produced by the photomultiplier, a scintillator is useless as a detector. The photomultiplier is essentially a fast amplifier, which in times of about 10 μs amplifies an incident pulse of visible light by a factor of 10 or more.

A photomultiplier consists of an evacuated glass tube with a photocathode at the entrance and several dynodes at the interior. The photons produced in the scintillator enter the phototube and hit the photocathode, which is made of a material that emits electrons when light strikes it. The electrons emitted by the photocathode are guided, with the help of an electric field, towards the first dynode, which is coated with a substance that emits secondary electrons, if electrons impinge upon it. The secondary electrons from the first dynode move towards the second, and so on.
The photocathode material most used is a compound of cesium and antimony (Cs-Sb). The material used to coat the dynodes is either

Cs-Sb or silver-magnesium (Ag-Mg).
A standard voltage divider network for a10dynodes photo-multiplier is shown in Figure 6.8.
The electron multiplication M in a photomultiplier can be written as:

(6.3) $$M = (\vartheta_1 \varepsilon_1)\ (\vartheta_2 \varepsilon_2)\ .....(\vartheta_n \varepsilon_n)$$

where:
n = number of dynodes
ε_i = number of electrons collected by the i-th dynode divided the number of electrons emitted by the (i-1) dynode
ϑ_i = number of electrons emitted by i-th dynode divided the number of electrons impinging upon i-th dynode
If ϑ_i and ε_i are constant for all dynodes, then:

(6.4) $$M = (\vartheta \varepsilon)^n$$

The quantity ε depends on the geometry. The quantity ϑ depends on the voltage between two successive dynodes and on the dynode material.
The dependence of ϑ on voltage is of the form:

(6.5) $$\vartheta = k\ V^a$$

Using Eq. (6.5) M becomes:

(6.6) $$M = \varepsilon^n (kV^a)^n$$

6.6 Amplifiers

6.6.1 Introduction

The heart of any spectroscopy, counting, or timing system is the amplifier. It provides the controls that select the analog

performance of the system. Linear, pulse-shaping amplifiers are used for energy spectroscopy, while timing amplifiers are used for timing measurements.
The principal functions of an amplifier in a pulse analysis system are mainly the following:
-toexpand the amplitude of pulses coming from the preamplifier (normally of the order of mV) into a range (volts) that can be measured with greater ease and accuracy.
-to shape the pulse from the preamplifier like a Gaussian,and to filter it to improve the signal to noise ratio and to prevent overlap.
Regarding the second point, it should be observed that the signal to noise ratio strongly depends on the forme of the pulses: the best theoretical pulse would be a cuspid, which is practically not realizable. A good compromise is given by the gaussian or the semigaussian pulse shaping, which can be realized by a sequence of differentiators and integrators (CR and RC circuits). Further,

to avoid overlap of pulses, the shaping time should be selected versus count rates.

6.6.2 RC pulse shaping

The term RC shaping applies to the use of resistors and capacitors as shaping network. In the following descriptions of these circuits a step function input is assumed, which is a good approximation for a pulse output from the preamplifier (Figure 6.7).
A CR differentiation filter (Figure 6.9) affects the decay of the pulse and corresponds to a high-pass filter, which attenuates the low frequency components.
A RC integration filter (Figure 6.10)affects the rise time of the pulse and corrseponds to a low-pass filter, which attenuates the high frequency components.
With CR-RC pulse shaping (Figure 6.11) in which a CR differentiator and an RC integrator are in cascade, the resulting

response removes both low- and high-frequency signal and noise components and significantly enhances the signal-to-noise ratio. For the majority of applications equal CR and RC time constant optimize the results.
The pulse-output from a CR-RC is called unipolar.
Bipolar pulses are produced by using double differentiation, i.e.

with CR-RC-CR pulse shaping in the main amplifier (Figure 6.12). Time constant of 0.5 to 12 μs are generally suited for all types of detectors.

All the above considerations have been made for a step pulse at
the input of the amplifier. In fact the output pulse from a preamplifier is characterized by a very short rise time (about 50 ns) and a long decay time (about 500 μs). That produces a small amplitude long negative pulse in the unipolar disposition

(undershoot with a decay time of about 500 μs;it corresponds to a first differentiation in the preamplifier and a second in the amplifier) and a positive undershoot in the bipolar disposition. This negative undershoot of the baseline in the unipolar pulse will produce a distortion in the amplitude of a second subsequent pulse (Figure 6.13), which can be canceled or reduced by the adding of one variable resistor to the differentiating circuit (pole-zero cancellation). It is extremely important that pole-zero cancellation be properly adjusted in any spectroscopy system. To compensate for the effect of base-line shift on a unipolar signal, also the baseline restoration (BLR) is used. This will restore the signal quickly to the baseline when an undershoot occurs.

6.6.3 amplifier signal versus count rates

As observed before, the signal to noise ratio is maximum for gaussian type pulses. Unipolar pulses from CR-RC shaping arethe most similar to gaussian pulses and are therefore characterized by the best energy resolution. For that reason unipolar pulses are used for low count rates ($\lesssim$ 1000 counts/s). They have, on the other hand the disadvantage of having a long negative undershoot, that rarely can be completely eliminated through P/Z or BLR circuits, and which will distort the pulse for high count rates. For that reason it is preferable to use the bipolar pulse for high counting rates, in spite of the worse energy resolution.
The phenomenon of decrease of maximum amplitude of pulses due to overlap to the undershoot of other pulses gives riseto a critical enlargement of the peak at the multichannel analyzer.
Also a more critical phenomenon can occurr, called pile-up. When two events arrive at the detector within the width of the spectroscopy amplifier output pulse, their respective pulses pile up to forme an output pulse of distorted amplitude. For detectors whose charge collection time is very short compared to the rise time of the amplifier pulse, an active circuits can be used, in the amplifier, called pileup rejection circuit which generates an inspection period immediately following every signal. If a second event occurs within this inspection period, an inhibit signal would be generated to gate-off the multi-channel-analyzer and thus discard the distorted amplifier output.Figure 6.14 shows for example the background reduction in a gamma ray spectrum as
pileup rejection is used.

An other possibility is to select the feedback resistor. Figure

6.15 shows how is varying the energy resolution of a planar HPGe detector at 122 keV.
A high class research amplifier should have the following characteristics:
gain range: continuously variable from 5 to 5000
gain drift: 0.0075%/ C
operating temperature: 0 to 50 C
pulse shaping: near gaussian shape: uinpolar and bipolar pulse
shaping time: from 0.25 to 12
restorer: active gated
pole-zero circuit
pile-up rejector

6.7 Single-channel analyzer
Due to the proportionality of the output pulses from an amplifier to the energy of incident particle or photon, theselection ofa range of energies of a nuclear event is equivalent to the selection of signal levels. This selection can be accomplished in a nuclear measurement system by the use of discriminators or single-channel analyzer.
A discriminator produces an output logic pulse if its input signal exceeds a preset threshold level.
A single-channel analyzer (SCA) produces an output logic pulse only if the peak amplitude of its input signal falls within the energy window that is established with two preset threshold levels.
Figure 6.16 shows three pulses that might be provided from a main amplifier to an integral discriminator. The first pulse has an amplitude less than the preset discriminator threshold and generates no output logic signal. Each of the last two pulses has sufficient amplitude to produce an output logic signal. The output signals are generated when the input signal crosses the discriminator threshold level. The time of the output response is then a function of the amplitude and rise time of the input signals.
Figure 6.17 shows the same three pulses provided from a main amplifier to a single channel analyzer. Only the second pulse satisfies the conditions necessary to produce an SCA output logic signal, because its amplitude lies between the lower-level discriminator and the upper level discriminator. Removal of the upper-level-discriminator from the SCA allows it to be used as an integral discriminator.
The technique used to produce the output logic signals from an SCA determines its classification. Non-timing units produces an SCA output pulse if the input signal is within the presetted windows. The output occurs when the input signal crosses the lower-level threshold. Timing SCAs produce SCA output logic signals that are precisely related in time to the occurrence of the event being measured. This time relationship implies that the time of occurrence of the SCA output signal is independent of the amplitude of the input signal, for a given rise time. Figure6.18 shows two pulses from a main amplifier and the response of a SCA. Although the amplitudes of the amplifier pulses differ, their peaks occur at approximately the same time. This method is called "zero-crossing" technique, and is widely used for timing single-channel analyzer. This technique utilizer the zero-crossing of the bipolar output signal from a pulse shaping amplifier to derive timing information, and uses the peak amplitude of the

pulse for the energy range information.
Figure 6.19 shows two bipolar pulses provided from a mainshaping amplifier. Both pulses meet the SCA window requirements. Each signal is generated when the corresponding input signal crosses the baseline.

6.8 Multichannel analyzers

6.8.1 Introduction

The multi channel analyzer (MCA) performs the essential functions of collecting the data, providing a visual monitor,and producing output, either final results of raw data for later analysis.
A basic MCA is shown as a functional block diagram in Figure 6.20. Analog pulses (customarily 0 to 10 V unipolar or bipolar from the amplifier) are digitized by a Wilkinson type ADC, and then stored in memory. The channel number is the memory address, and is proportional to the input signal voltage. Each pulse is digitized and a count added to the appropriate memory location, so that a spectrum of number of pulses vs voltage is obtained. The range of channels and of ADC resolution is a minimum of 256 to a maximum of 16348.

6.8.2 Analog-to-digital converter characteristics

The basic digitizing of an input analog signal is performed by the analog-to digital (ADC) converter of the Wilkinson type and successive approximation.
The Wilkinson type ADC digitizes a pulse by charging a capacitor to the amplitude of the input, and then discharging the capacitor at a constant rate. During the discharge time a crystal controlled pulse train is counted in a register. When the ramp has returned to the baseline, the number in the register represents the input signal pulse height. The details of the operation of the Wilkinson ADC is illustrated in Figure 6.21 and 6.22.
The lower-level discriminator (Fig. 6.21 a and 6.21 b),which threshold is set just above the noise level, is usedto recognize the arrival of the amplifier output pulse. When the input pulse rises above the lower-level discriminator threshold, the input linear gate is open and the rundown capacitor is connected to the input (Fig. 6.22 b). Thus, the capacitor is forced to charge up so that its voltage follows the amplitude of the rising input pulse (Fig. 6.21 c). When the input signal has reached its maximum amplitude and begins to fall the linear gate is closed and the capacitor is disconnected from the input (Fig. 6.22 b). At this point the voltage of the capacitor is equal to the maximum amplitude of the input pulse. Following peak amplitude detection, a constant current source is connected to the capacitor to cause a linear discharge (rundown) of the capacitor voltage (Figs. Fig. 6.22 b). At the same time, the address clock is connected to the address counter (Figs. 6.21 d and 6.22 b) and the clock pulses are counted for the duration of the capacitor discharge. When the voltage of the capacitor reaches zero, the counting of the clock ceases. Since the time for linear discharge of the capacitor is proportional to the original pulse amplitude, the number N recorded in the address counter is also proportional to the pulse amplitude.
During the memory cycle (Figs. 6.21 e and 6.22 c) the address N is located in the histogramming memory, and one count is added to the contents of that location. The value N is usually

referred to as the "channel number".
In conclusion, and considering the nuclear detection and analysis from the beginning (for example radioactive source) to the end (multichannel analyzer), it may be observed that the energy of the incident particle or photon is converted, in the amplification chain, in an electric pulse with proportionalamplitude. The multichannel analyzer finally sortes the pulses into channels, according to amplitude, to yield a histogram representing counts versus pulse height, and preserving a linear

relationship. A "spectrum" of the analyzed nuclear process is finally obtained (Figure 6.23).
The most important parameters and characteristics of a MCA are:
- the maximum number of channels, which is in some way connected to the resolution of the system, in the sense that more channels means more points per unit of energy; of course the usefulness of using more channels is depending on the complexity of the spectrum; submultiples of the maximum number of channels are in general at disposal, giving rise to different "ADC conversion gains". For example, with 8192 conversion gain and an 8 volt input signal, the resolution is about 1 mVolt per channel.
- linearity, both differential and integral, which indicates the

errors in the "calibration" of the spectrum, i.e. in correlating channel numbers to energy values;
- dead time: because of the finite amount of time required to analyze each pulse, the MCA is "dead" during the pulse conversion time. That is, it cannot respond to another pulse during that time. The total dead time is the sum of three terms: the time protection, which indicates the time after one pulse in which the entrance of the MCA is paralized, the conversion time, which is depending on the time required for the analog-digital conversion and is depending on the linear ramp pulse, and, finally, the registration time.
To compensate for this dead time, the MCA's live time clock is gated off during the dead time intervals, so that only "live" time is recorded.
For the Wilkinson ADC, the measurement time of the MCA contributes a dead time as expressed in Equation

(6.3) $$T_M = (N_c / f_c) + T_{mc}$$

where:
N_c = the channel number
f_c = the clock frequency
T_{mc} = the memory cycle time.

6.8.3 multichannel scaling (MCS)
the MCS - analysis yields a histogram representing count rate

versus time. In the MCS mode, pulsesare stored in successive channels for a predetermined period of time, called the dwell time. At the end of each dwell time period, collection begins in the next memory channel. Each memory channel is thus sequentially selected as a function of time. MCS analysis finds usein several applications involving the study of the distribution of events as a function of time.

7. ALPHA, BETA, X AND GAMMA-RAY SPECTROSCOPY

7.1 Introduction

By means of a simple electronic chain, composed by a detector, a preamplifier, an amplifier and a multichannel-analyzer, as shown in Figure , the spectral distribution can be measured of charged particles, of ionizing radiation and of neutrons. The characteristics of the spectra depend mainly on the detector, and then on the other components of the chain.

7.2 Alpha-ray spectroscopy

Alpha-rays can be measured by means of a ionization chamber or a gas proportional detector with very thin mica window, or with a Si charged particle detector, which is a wafer of Si having surface contacts forming a p-n junction. These contacts may be surface barriers or may be junction contacts as in the modern high-performance passivated implanted planar silicon (PIPS) detector. A bias voltage is applied in the reverse direction to establish an electric field across the device. The reverse bias acts to form a depletion region in which there are no free charges. To function as a particle detector, the depletion region should be thicker than the penetration range of particles being detected, for example about 32 μm for 6 MeV alpha particles in silicon.
A spectrum from Th^{232} emitting alpha rays from 5.6 to 6.1 MeV is shown in Figure 7.1.
In an alpha spectrum the interpretation of the spectrum is very easy, because there are no secondary effects or partial losses of energy from the particle, but only "full energy" peaks.

7.3 Beta-ray spectroscopy

The detectors for alpha particles may also be employed for the detection of beta particles, considering the zero range of beta particles. For example PIPS detectors may be used of adequate thickness: beta particles of maximum energy of 100 keV need about 80 m of Si, and of 1 MeV about 800 m of Ge, and 2500 of Si.
For example the beta spectrum of Bi^{207} between 0 and about 2 MeV is shown in Figure 7.2.
Also the interpretation of a beta spectrum is in general easy, and any beta particle or electron loses its full energy in the detector.

7.4 X-ray spectroscopy

X-rays, having energy between about few keV and about 100 keV, may be detected by means of a gas proportional detector,a Si-cooled semiconductor detector, and a HPGe-detector, according to the energy range and to the energy resolution required.
Gas proportional detectors, filled with A, Kr, Xe, Ne, have a energy resolution of about 18% at 5.9 keV, and are suited for detection of X-rays of energy till about 30-35 keV, depending on the gas filling and its pressure (see for example Figures 7.3 and 7.4, giving the absorption curves of A and Kr at 1 atm .
The minimum detectable energy is depending on the window transmission (see Fig. 7.5) .Flux windowless proportional counters are also available.
A typical X-ray spectrum collected with a Xe-filled proportional counter is shown in Figure 7.6.

Cooled Si-detectors of adequate thickness (few mm) are suited for detecting X-rays in the range of few keV (depending on the entrance window) to about 100 keV, with an energy resolution of about 160 eV at 5.9 keV, corresponding to about 2.7% and about 400 eV at 100 keV, corresponding to about 0.4% .
A typical X-ray spectrum collected with a semiconductor detector

is shown in Figure 7.7.
Also room temperature HgI_2 -semiconductor detectors may be used for detecting X-rays, with an energy resolution of about 250-300 eV.
Cooled HPGe-detectors are also suited for the analysis of X-rays of any energy, starting from 4-5 keV, depending on the Be-window.

The interpretation of a X-ray spectrum is,in general, not difficult, but depending on the detector and its energy resolution.
In the emission of K-X-rays from an element, two lines are emitted, K_α and K_β in an intensity ratio of about 6 to 1. The two lines are relatively close, and are clearly separate only with a high-resolution detector. In the low-energy region the photoelectric effect is largely prevailing to the other and there are only the "full energy" peaks. At higher energy there is also with increasing probability Compton effect, giving rise to a continuous distribution of pulses (see Section 7.5 for more details on these effects) and a Compton peak.

7.5 Gamma-ray spectroscopy
In the case of gamma rays in the region between about 100 keV and 10 MeV, all effects of interaction between photons and matter may be considered: besides photoelectric effect, Compton and Rayleigh scattering and pair production.
After a photoelectric effect the secondary electron takes the full energy of the incident photon minus the binding energy of the atom (see Eq.3.1) . The excited atom deexcite by emitting and

an Auger electron (which will be of course lose its energy in the detector),or a X-ray, which will be also absorbed in the detector with high probability. Finally, a peak is produced in the MCA corresponding to the full energy of the incident photon. If the X-ray is escaping from the detector volume, a second peak may appear in the MCA, having energy $E_0 - E_K$. InaCompton event, the total energy of the incident photon is shared between the secondary electron and the Compton photon; the secondary electron, which energy may vary from zero to a maximum value given by:

(7.1) $$E_{MAX} = E_0 - E_0 / \left(1 + \frac{2h\nu}{m_0 c^2}\right)$$

will be certainly detected, the Compton photon can escape the detector.Inthis case a Compton continuous distribution will appear from zero to a maximum energy given by Eq.(7.1), which is called Compton edge.
Only in the case of a secondary photoelectric interaction of the

Compton photon there will be a contribution to the full energy peak.
In the case of high energy photons ($E >> 1022$ keV) the situation is still more complicated, due to the pair production and

possible escape of one or two 511 keV photons. For that reason, for a gamma-ray of energy E_γ, peaks at E_γ (full-energy) at E_γ - 511 keV and at E_γ -1022 keV are expected. Moreover, Compton continuum and Compton peaks of all these peaks are present (see Figure 7.8).
It should be finally observed that radiation emitted from the source may interact, besides with the material of the detector, also with the source collimator material, the shielding material, the air, the detector and so on, giving rise to spurious peaks, which should be considered, especially when very low radiation levels should be measured.

8. Detectors and Electronics control and maintenance
Let us consider again a detector with a simple Electronic chain, composed by a high-voltage generator, a preamplifier, an amplifier, a single-channel analyzer, a timer-scaler or a ratemeter or

a multichannel-analyzer. The Electronics is plug in a low-voltage box, providing generally 0, +6, +12 and +24 Volts (Figure 8.1).

To test every part of the electronic chain, an oscilloscope should be employed, and a voltmeter and a pulser are very useful.

After connecting all parts of the Electronics, and positioning a radioactive source in front of the detector, the pulse at the output of the preamplifier or photomultiplier should be checked. In the first case a pulse of about mV amplitude, a short rise time, less than 1 s, and a decay constant of hundreds of s should be expected, in the second case a pulse a fractions of Volts to Volts with a short rise time and a decay constant of tens to hundreds of s. If the pulse at the output of the preamplifier is completely absent, the high-voltage and the low-voltage generators should be controlled, and the connection. If all is in order, one can try to change the preamplifier or, if available, the detector. The preamplifier can be tested alone, by using a pulser. The output of the pulser,with appropriate amplitude, should be introduced into the test input of the pA. If there is no output from the preamplifier, then the pA is possibly not working.
If the pulse at the output of the preamplifier is present, is
correct,and is clearly correlated to the source (which can be tested by removing the source),thenthe pulse shape at the output of the amplifier should be checked, which has to be unipolar or bipolar,ofthe gaussian type,withan amplitude of Volts and ri-setimeand decrease time of the order of s. If unipolar, the undershoot contribution should be eliminated by manipulating the pole-zero and/orthe base line-restorer.If a monoenergetic strong enough radiationis emitted by the source, this radiation should be clearly visible in the oscilloscope as a clear curve (Figure

8.2). Further,looking at the low voltage position of the oscillo-scope, inthe range of ms to hundreds of ms, not too much noise should be visible, both of low-and of high frequency.
If thepulse at the bipolar output of the amplifier is present andis correct, and no noise is present, then the pulse at the output of the single channel analyzer can be controlled with the oscilloscope, which is a logic pulse of 5 Volts amplitude with very short rise and decay time. If no pulse is present at the single-channel analyzer output, then the upper and lower level of the SCA should be tested in relation to the pulse to be selected in the amplifier, starting working with the SCA in the discriminator position with a very low level, moving the level and controlling the logic signal at the output.

Finally, the spectrum can be collected at the multichannel

analyzer, and the energy resolution of the lines can be checked. If this last parameter is not correct, then possibly the amplifier output is not correct (uncorrect constant differentiatiotion and integration times, pole-zero is not working well, BLR is out, or the count rate is too high, giving rise to a strong pile-up. In this last case, or an amplifier with pile-up rejection is available, or a bipolar pulse should be used, or the source should be taken away.

REFERENCES

M. Giannini, R. Cesareo: "Rivelazione ed analisi delle radiazioni

nucleari", University of Rome, 1981/82.
Canberra: Laboratory Manual for Nuclear Sciences, USA 1988
O.C. Allkofer: "Teilchendetektoren", Verlag K. Thiemig KG, Muenchen, 1971
Canberra Edition Seven, Meriden, USA
Reuter-Stokes: X-Ray proportional counters, Cleveland, Ohio, USA 1982
EG&G Ortec: "Detectors and Instruments for Nuclear Spectroscopy", Oak Ridge,TN,USA,1991
LND, Inc. Designers & Manifacturers of Nuclear Radiation Detectors, Oceanside, NY, USA, 1990.
NBSIR 82-2550-A: "Stopping power and ranges of electrons and positrons; U>S> Dept. of Commerce, Nat. Bureau of Standards, Dec. 1983.
J.H.Hubbell: Photon cross sections, attenuation coefficients and energy absorption coefficients from 10 keV to 100 GeV; NSRDS-NBS 29, Nat. Bur. Stand. 1969.

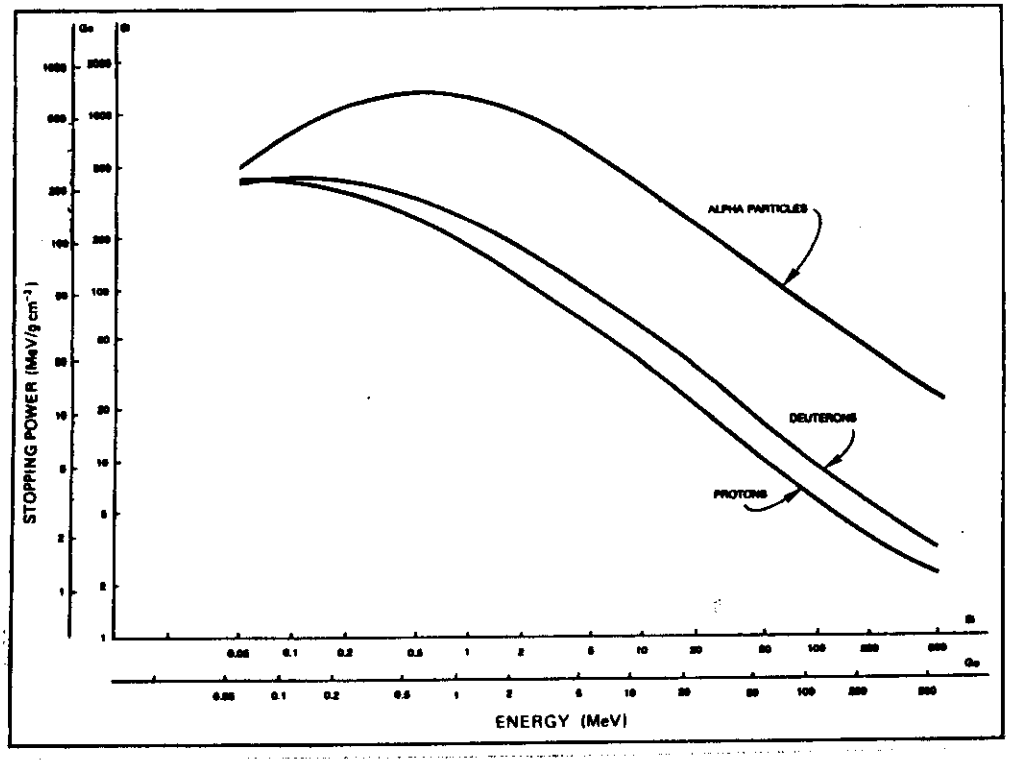

Figure 2.1 - Stopping power vs. energy for protons, deuterons and alpha particles in Si and Ge.

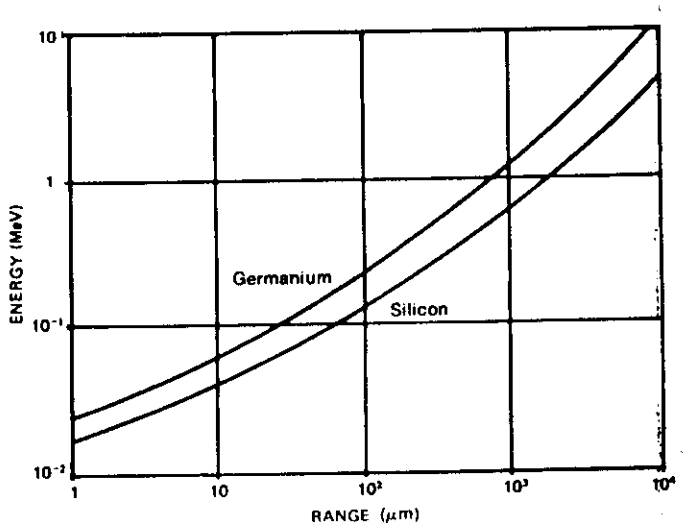

Figure 2.3 - Zero transmission range vs. energy for electrons in Si and Ge.

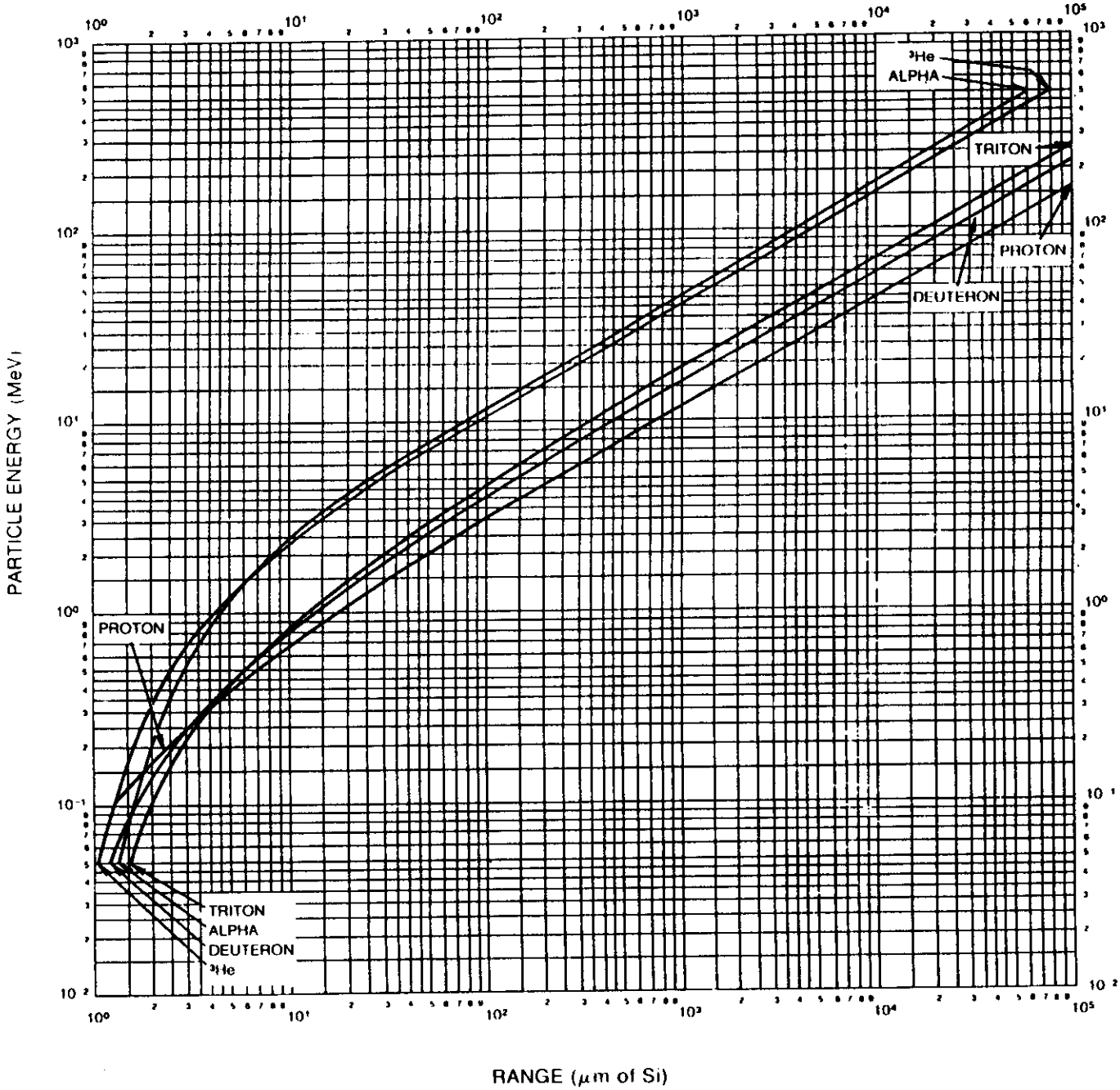

Figure 2.2 - Range vs. energy curves for charged particles in Si

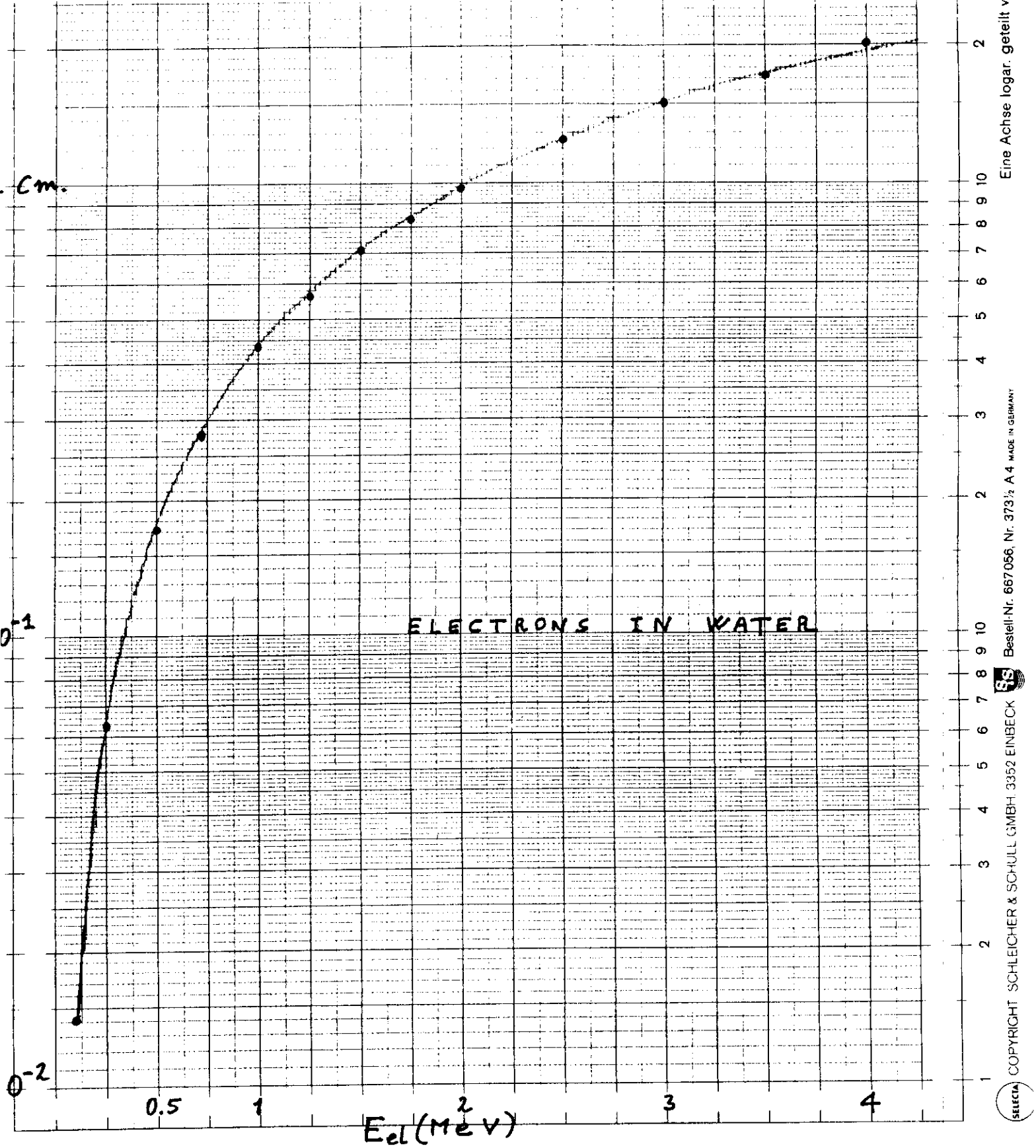

Fig. 2.4 - Range (in cm) of electrons in water.

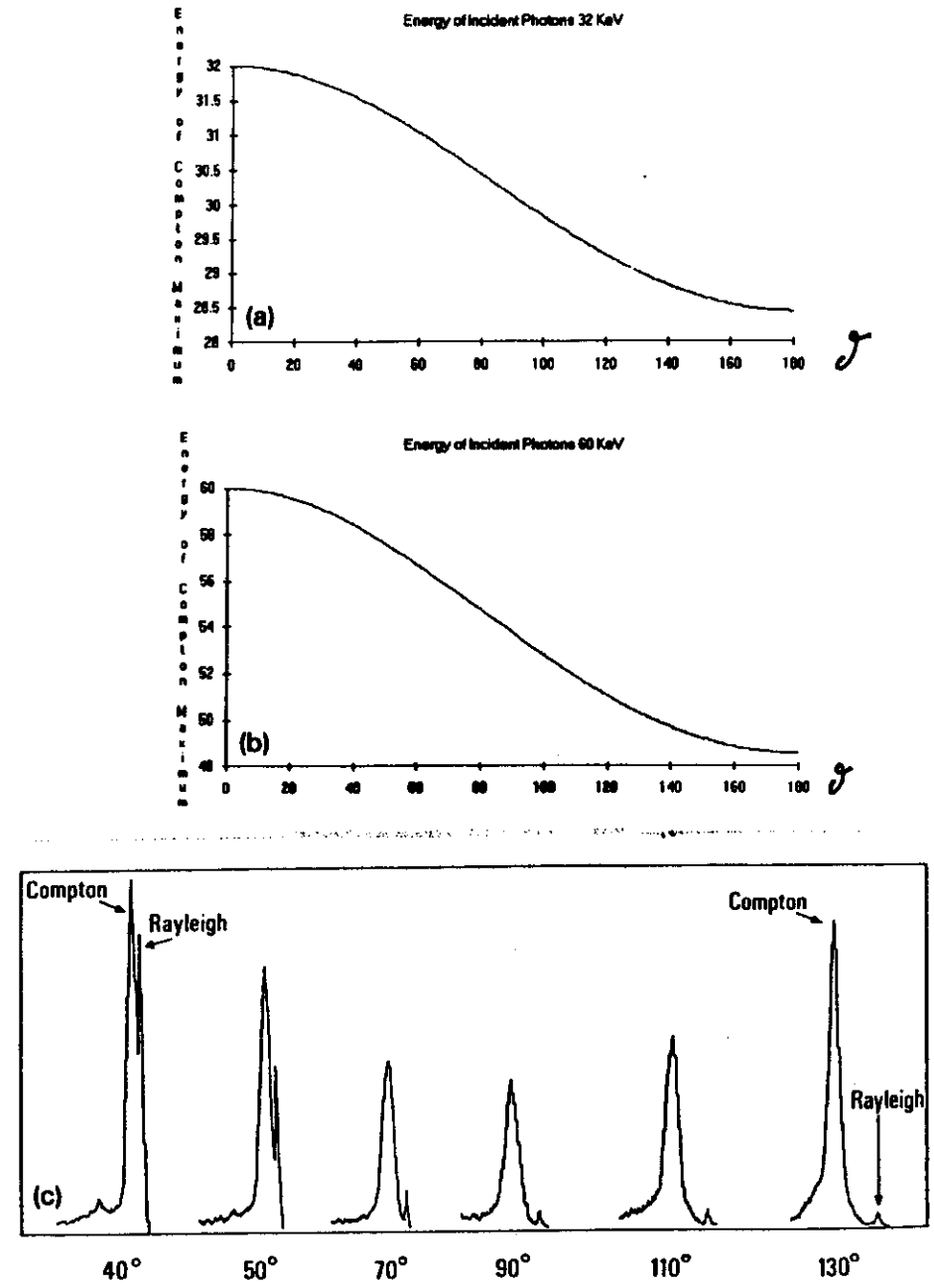

Figure 3.1 - Energy of Compton scattered photons vs. scattering angle for E_γ = 32 and 60 keV incident energies, and scattered spectra produced by 59.6 keV gamma-rays at various angles detected with a high resolution detector.

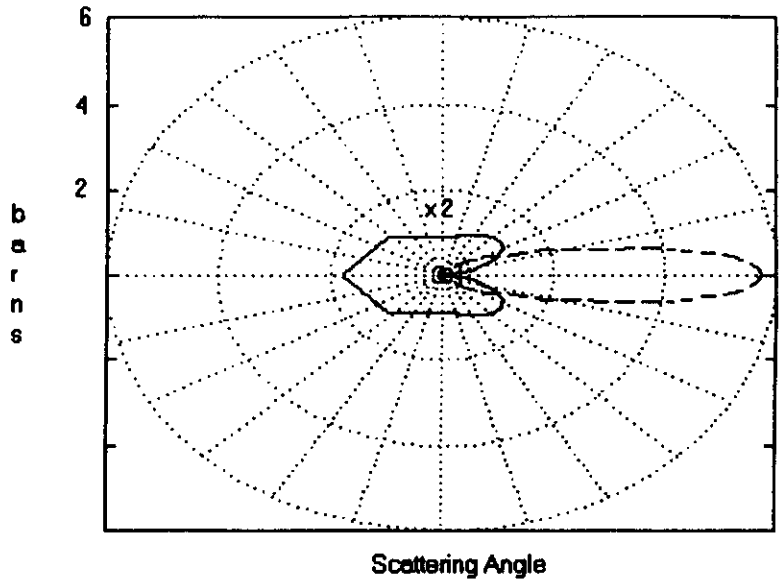

Figure 3.3 - Differential cross section for Compton and Rayleigh scattering (dotted line) in water, for E_0 = 20 keV.

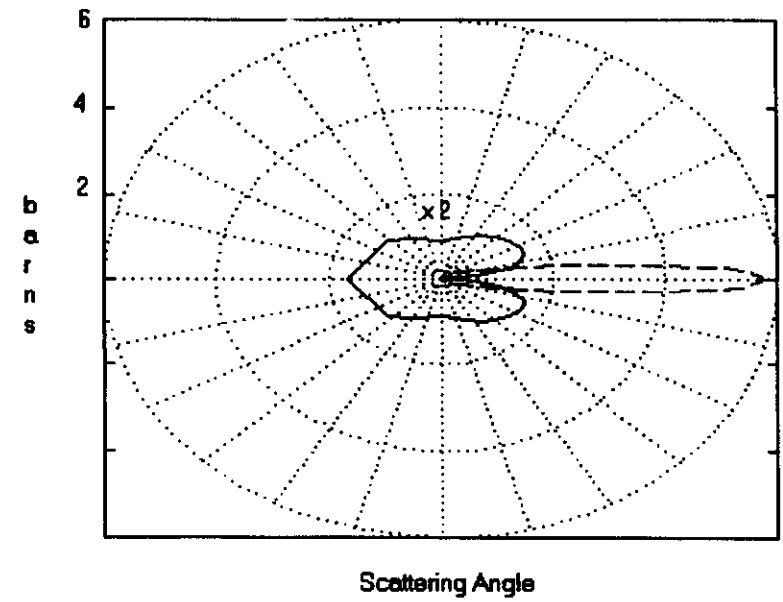

Figure 3.4 - Differential cross section for Compton and Rayleigh (dotted line) scattering in water, for E_0 = 40 keV.

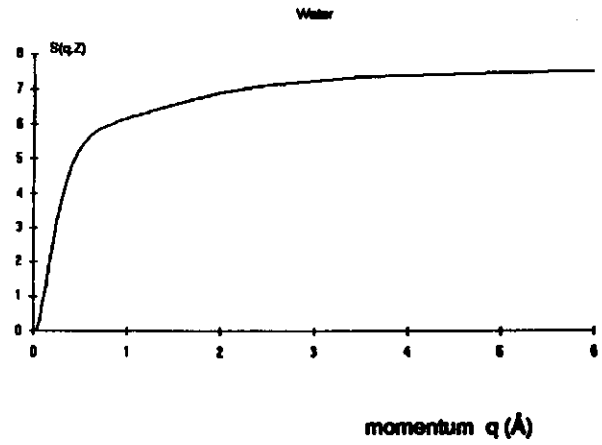

Figure 3.2 - Incoherent scattering function S(q,Z) versus momentum q for Z = 7.5. Theoretical values.

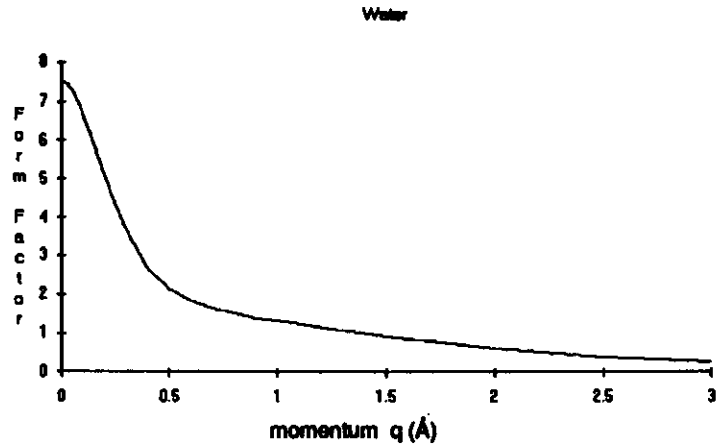

Figure 3.5 - Atomic form factor F(q,Z) for water versus momemtum Theoretical values.

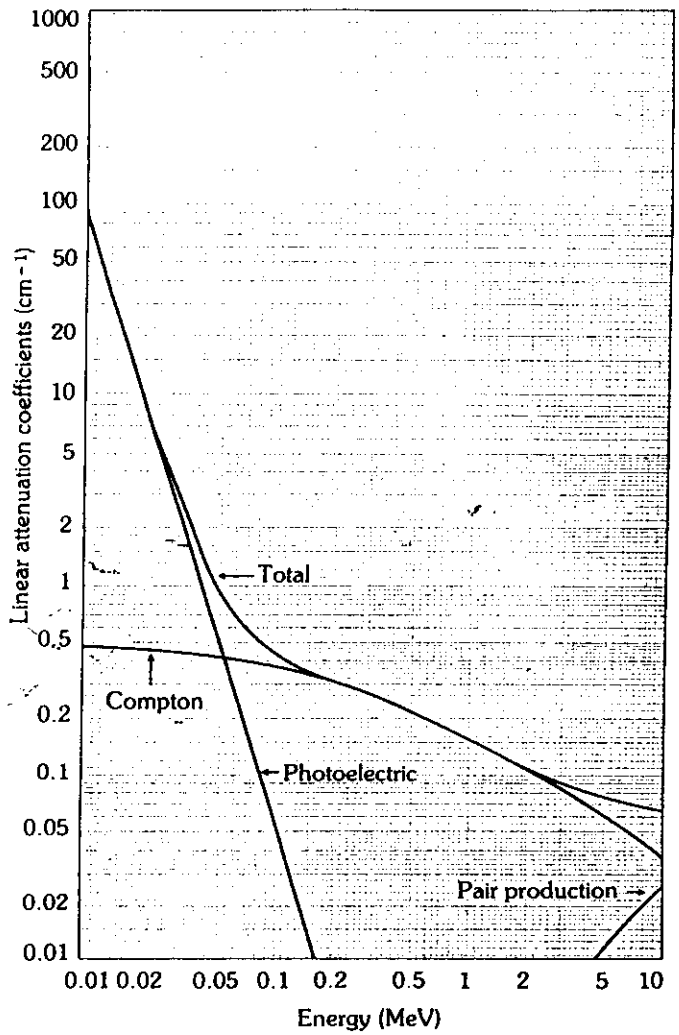

Figure 3.6 - Linear attenuation coefficients vs. gamma ray energy for Si.

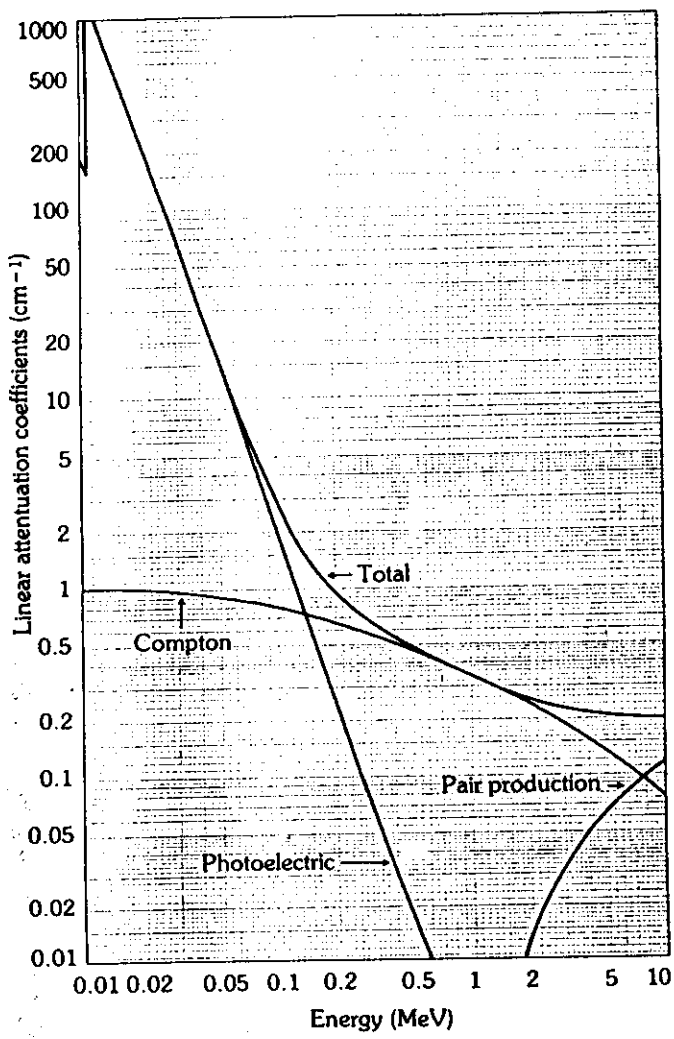

Figure 3.7 - Linear attenuation coefficient vs. gamma ray energy for Ge.

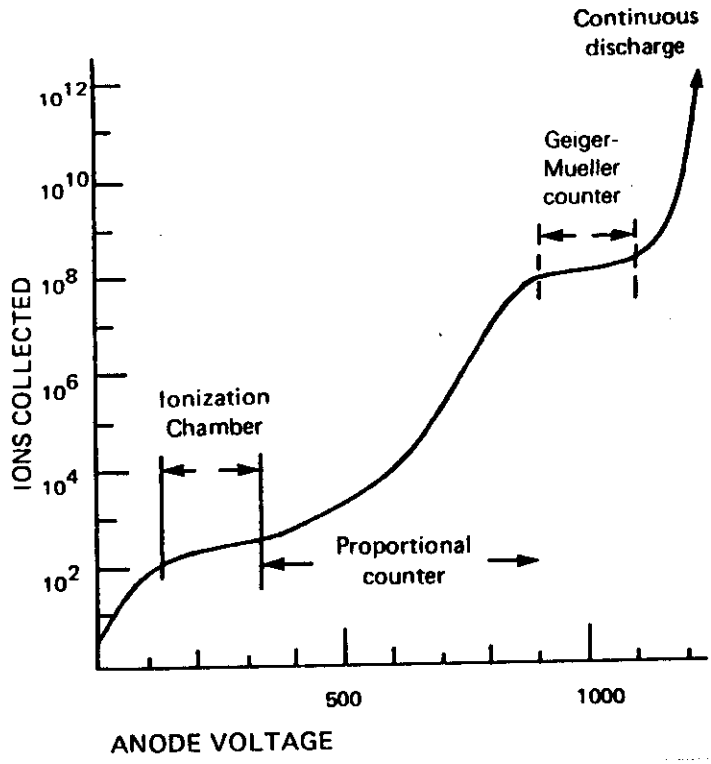

Figure 5.1 - Gas- detector output (number of collected ions) vs. anodevoltage. The different regions related to the ionization chamber,proportionaldetector andGeiger-Mullercounterare clearly visible.

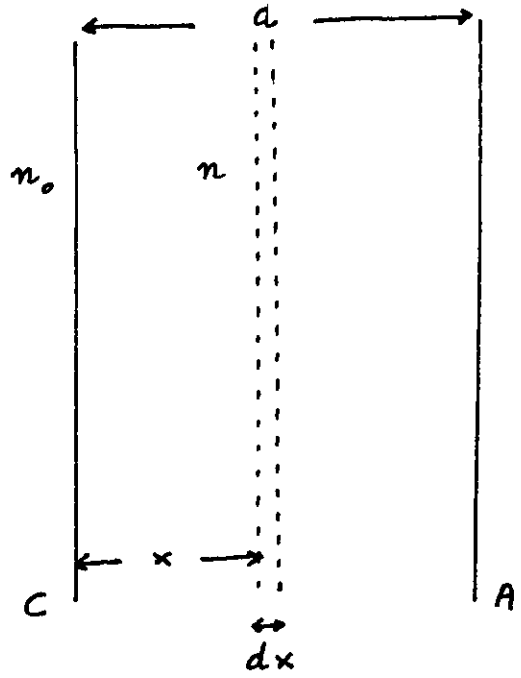

Figure 5.2 - Charges in an electric field.

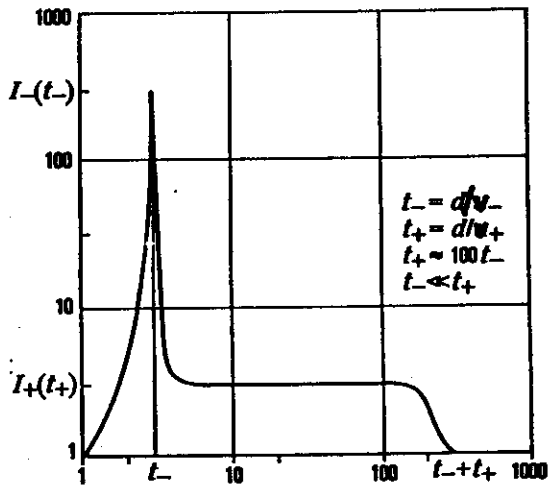

Figure 5.3 - Current of electrons and ions in a gas detector

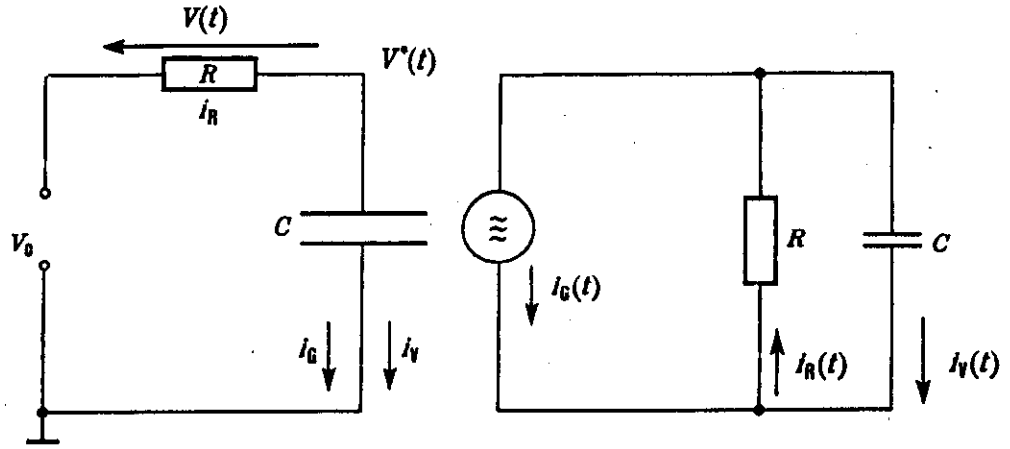

Figure 5.4 - Equivalent circuit for a gas detector

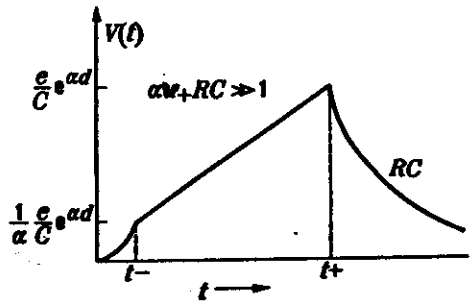

Figure 5.5 - Pulse curve vs. time in a gas detector when $RC \gg \frac{1}{\alpha v_+}$

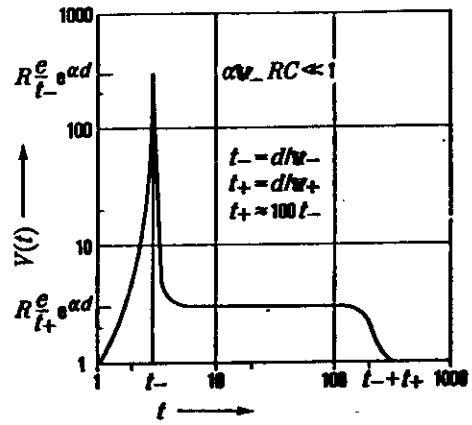

Figure 5.6 - Pulse curve vs. time in a gas detector when $RC \ll \frac{1}{\alpha v_-}$

Figure 5.7 - Typical ionization chamber

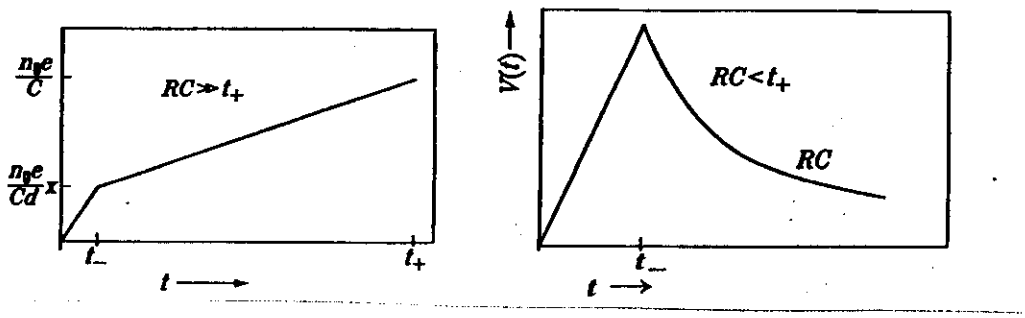

Figure 5.8 - Pulse curve vs. time for a ionization chamber in the case $t_- < RC < t_+$.

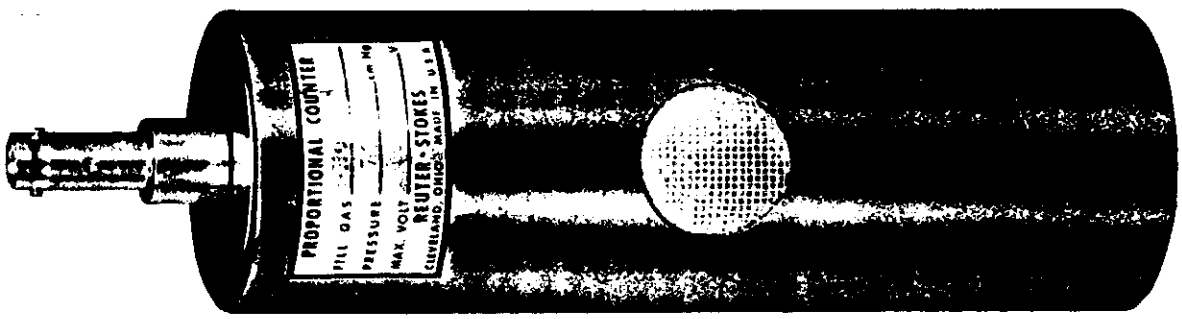

Figure 5.9 - Typical gas proportional detector.

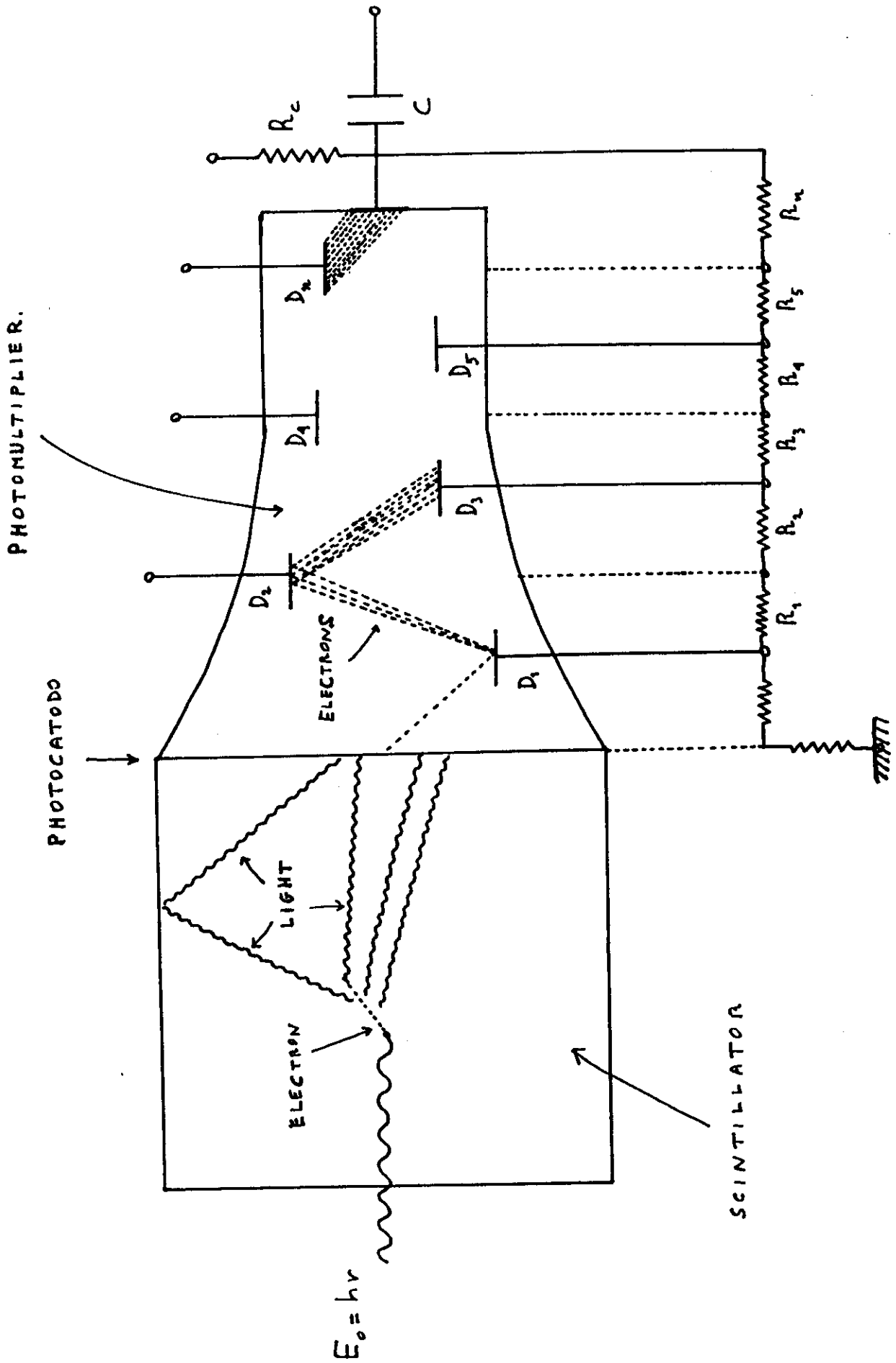

Figure 5.10 - Scheme of a typical scintillator with relative photomultiplier.

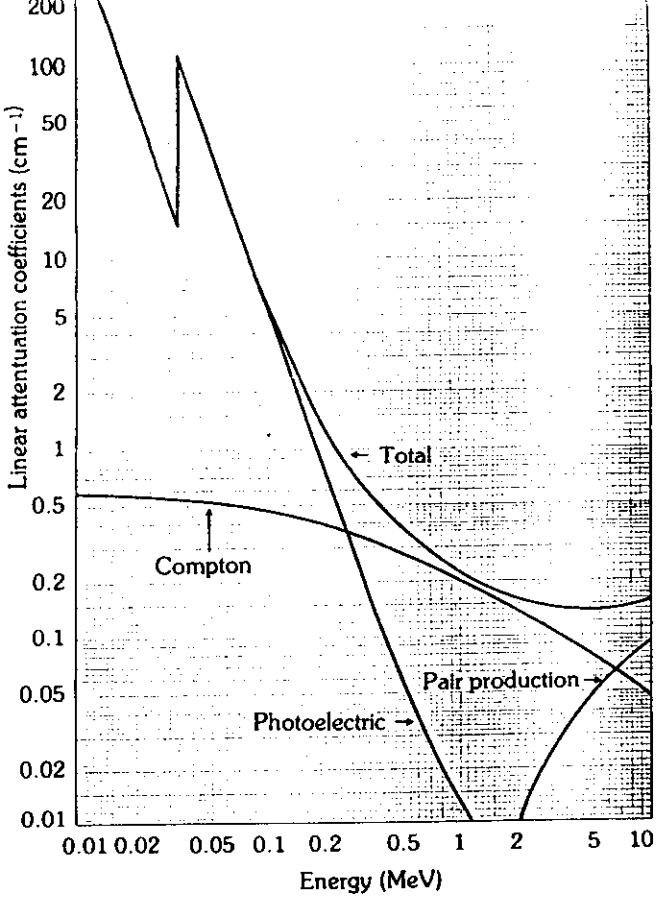

Specific mass = 3670 kg/m³
Atomic Number: Z(I) = 53
Z(Na) = 11
Electron Binding Energies:
K-edge (I) = 33.17 keV
L_I-edge (I) = 5.19 keV
L_{II}-edge (I) = 4.85 keV
L_{III}-edge (I) = 4.56 keV
Average K X-Ray Energy (I) = 29.2 keV

Figure 5.11 - Attenuation coefficient vs. energy of NaI.

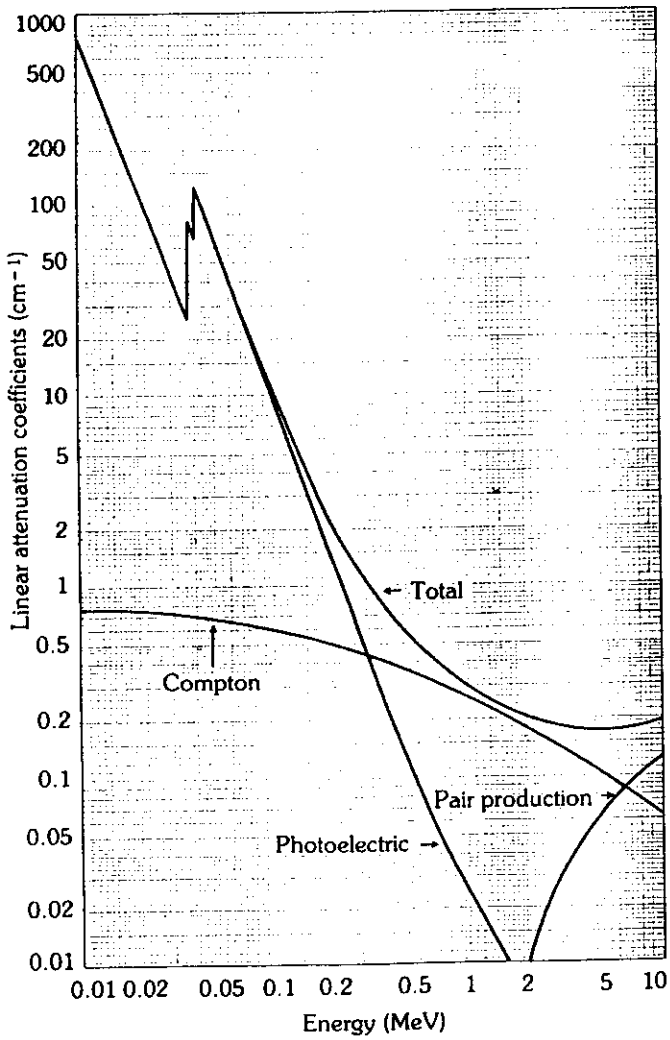

Specific mass = 4510 kg/m³
Atomic number: Z (I) = 53
Z (Cs) = 55
Electron Binding Energies:
K-edge (I) = 33.17 keV
K-edge (Cs) = 35.98 keV
L_I-edge (Cs) = 5.72 keV
L_{II}-edge (Cs) = 5.36 keV
L_{III}-edge (Cs) = 5.01 keV
Average K X-Ray Energy (Cs) = 31.6

Figure 5.12 - Attenuation coefficient vs. energy of CsI.

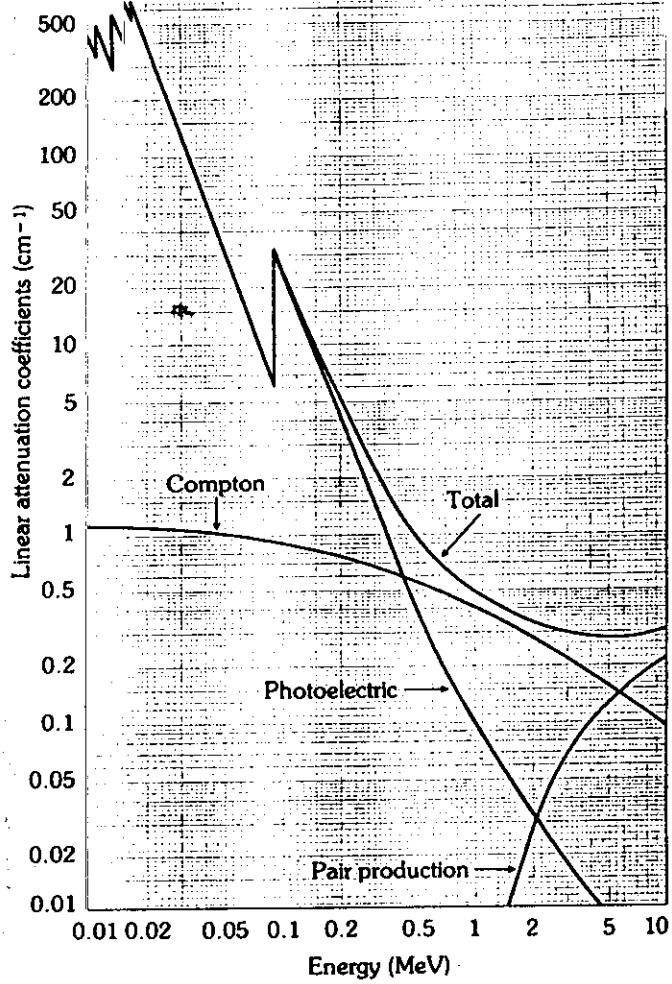

Specific mass = 7130 kg/m³
Atomic number: Z (Bi) = 83
Z (Ge) = 32
Electron Binding Energies:
K-edge (Bi) = 90.53 keV
L_I-edge (Bi) = 16.39 keV
L_{II}-edge (Bi) = 15.71 keV
L_{III}-edge (Bi) = 13.42 keV
K-edge (Ge) = 11.10 keV
Average K X-Ray Energy (Bi) = 78.9 keV

Figure 5.13 - Attenuation coefficient vs. energy of BGO.

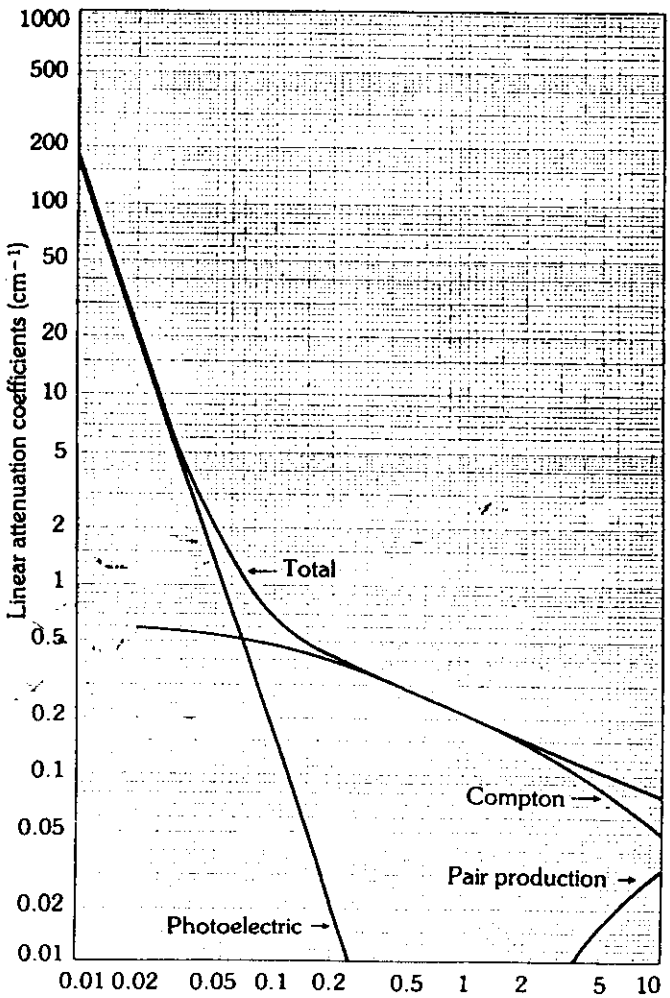

Specific mass = 3190 kg/m³
Atomic number: Z (Ca) = 20
Z (F) = 9
Electron Binding Energies:
K-edge (Ca) = 4.04 keV
K-edge (F) = 0.69 keV
Average K X-Ray Energy (Ca) = 3.7 keV

BaF_2

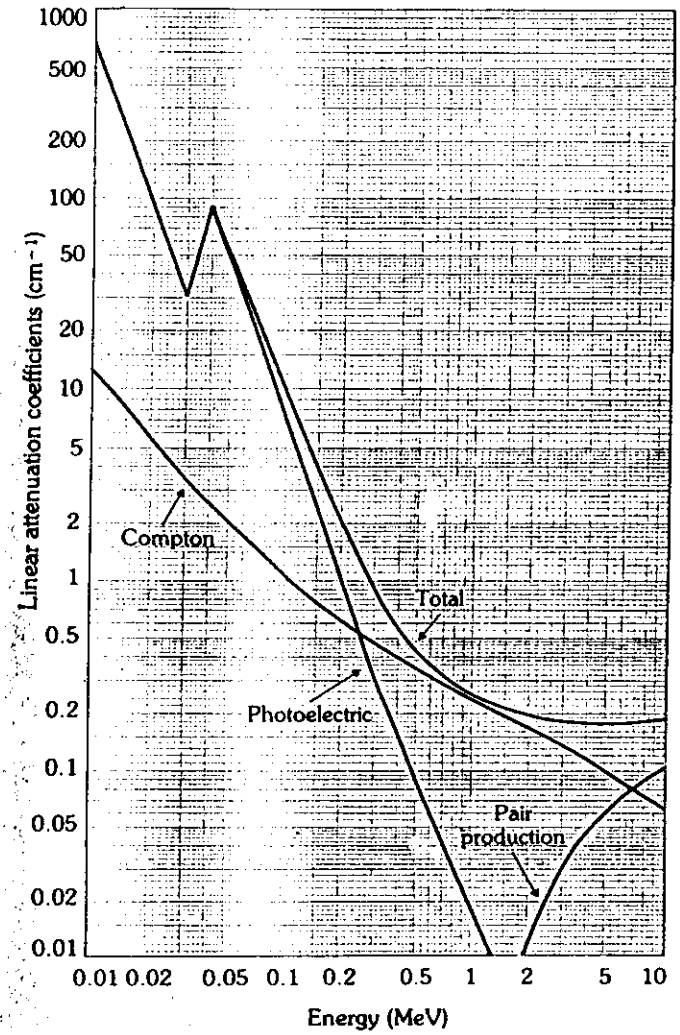

Specific mass = 4880 kg/m³
Atomic number: Z(Ba) = 56
Z(F) = 9
Electron Binding Energies:
K-edge (Ba) = 37.44 keV
L_I-edge (Ba) = 5.99 keV
L_{II}-edge (Ba) = 5.62 keV
L_{III}-edge (Ba) = 5.25 keV
K-edge (F) = 0.69keV

Figure 5.15 - Attenuation coefficient vs. energy of BaF_2 .

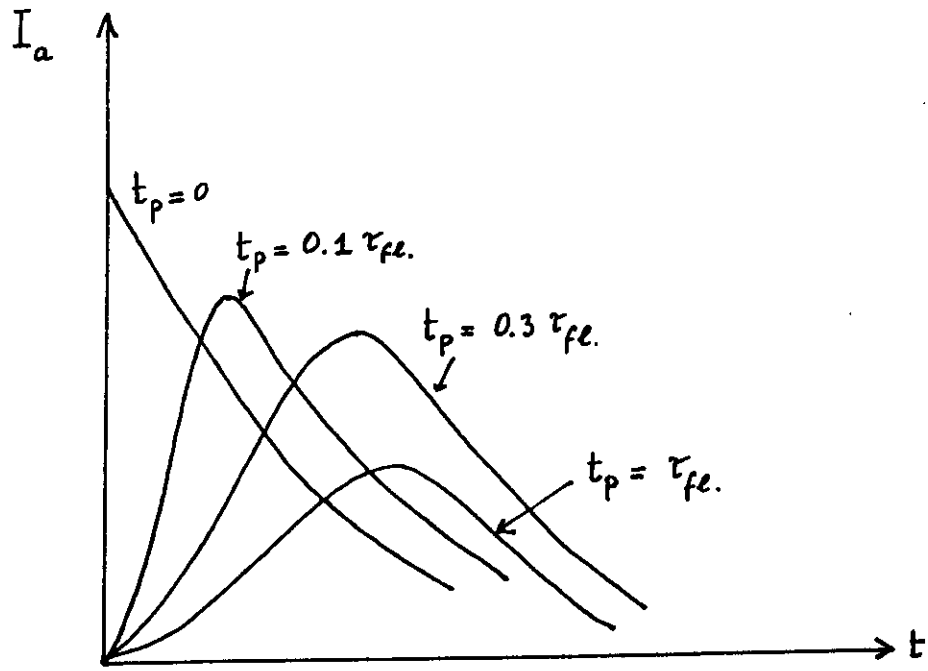

Figure 5.16 - Anodic current vs. fluorescent constant for a scintillator plus photomultiplier.

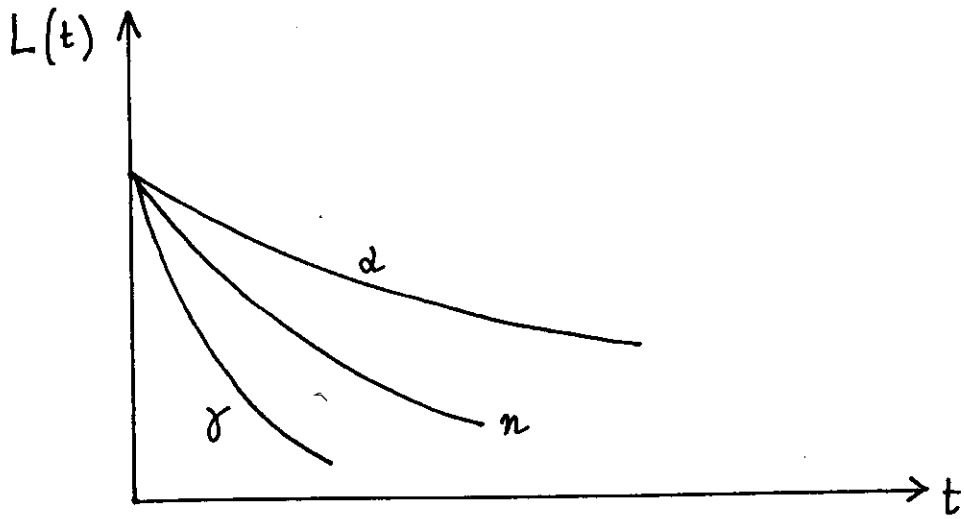

Figure 5.17 - Anodic current vs. type of incident particle, at constant transit time, for a scintillator plus photomultiplier.

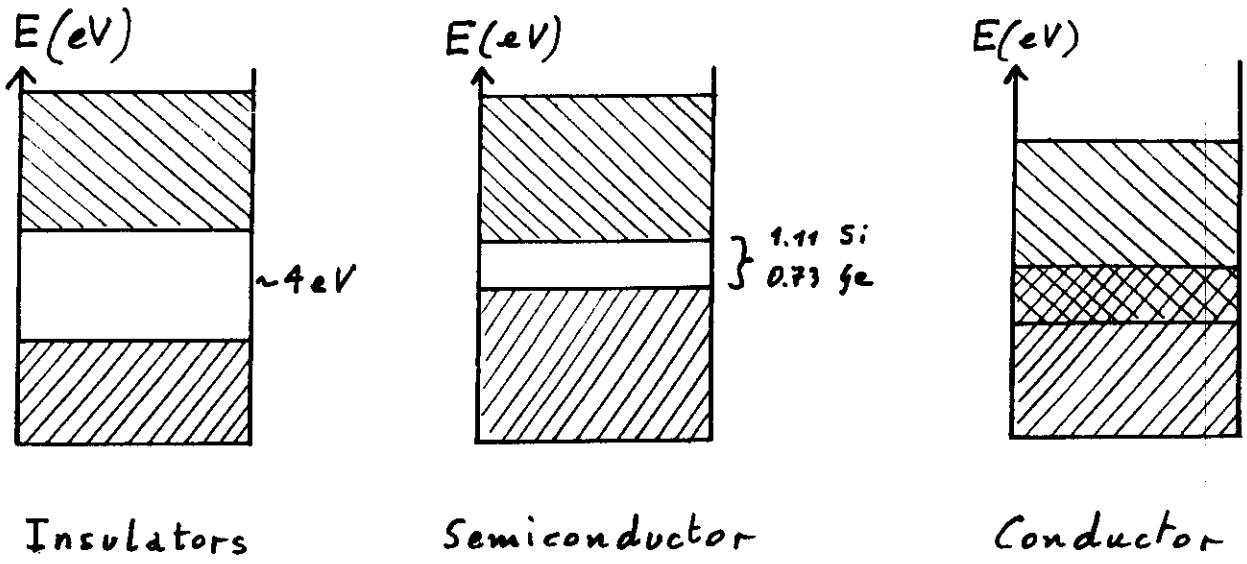

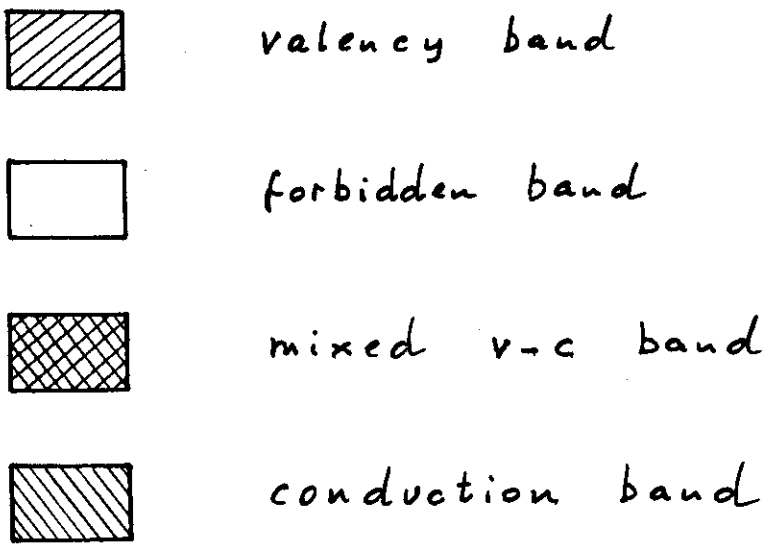

Figure 5.18 - Band of valence and of conduction for insulators, conductors and semiconductors.

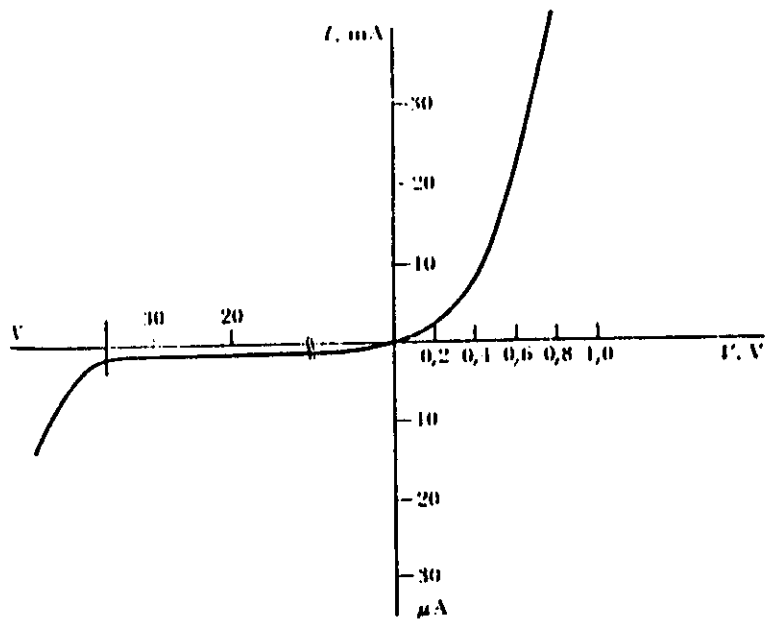

Figure 5.19 - Current vs. voltage for a p-n junction.

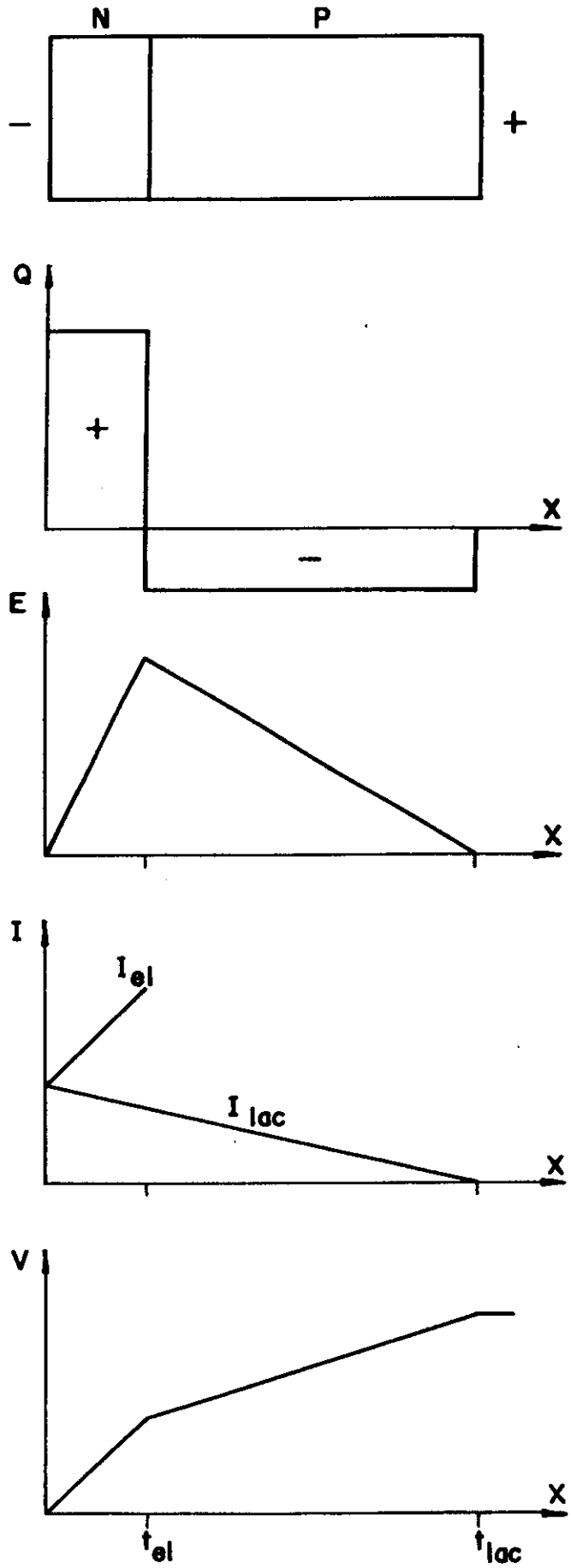

Figure 5.20 - Distribution of charges, current and voltage in a semiconductor material.

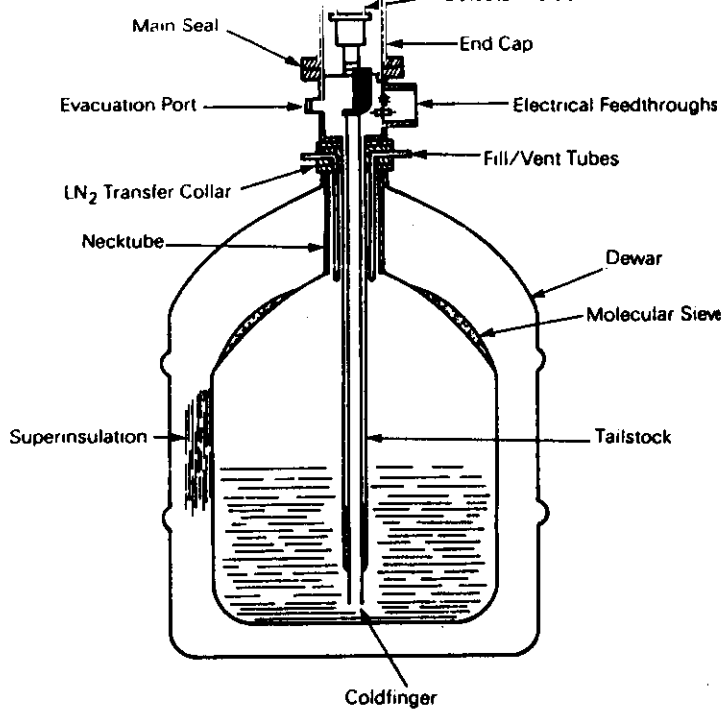

Figure 5.21 - Cryostat for the refrigeration of a cooled semiconductor detector.

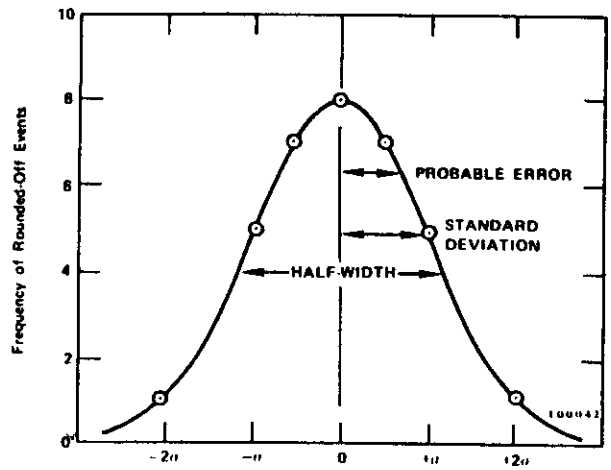

Figure 5.22 - For the definition of the full width at half maximum (FWHM) of a peak.

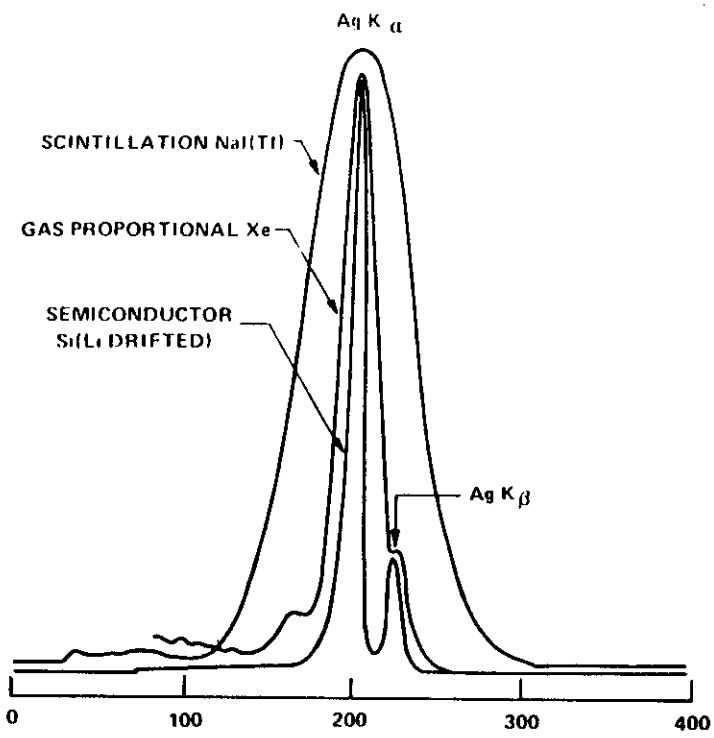

Figure 5.23 - Energy resolution vs. energy of different detectors for the silver X-rays (22 keV).

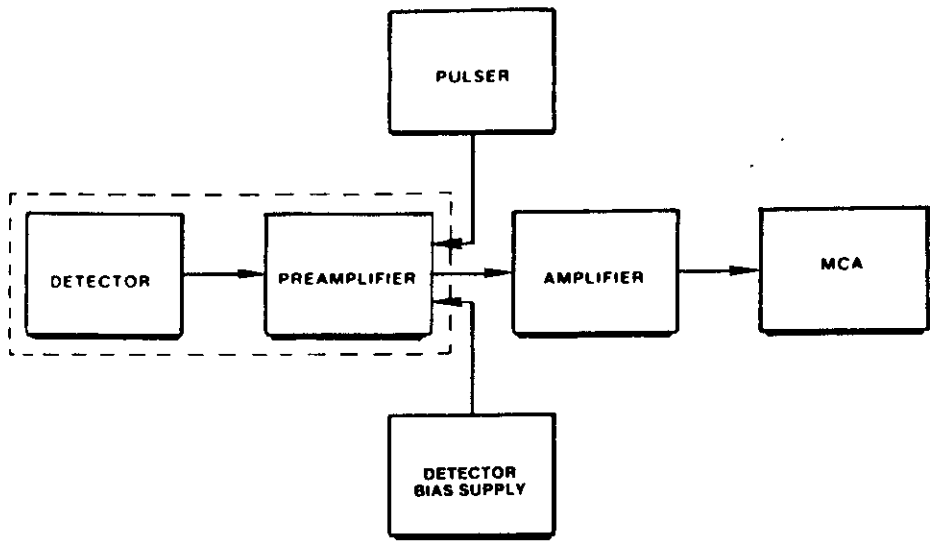

Figure 6.1 - A simple spectrometry system, characterized by a detector,preamplifier,amplifier and multi-channel-analyzer.

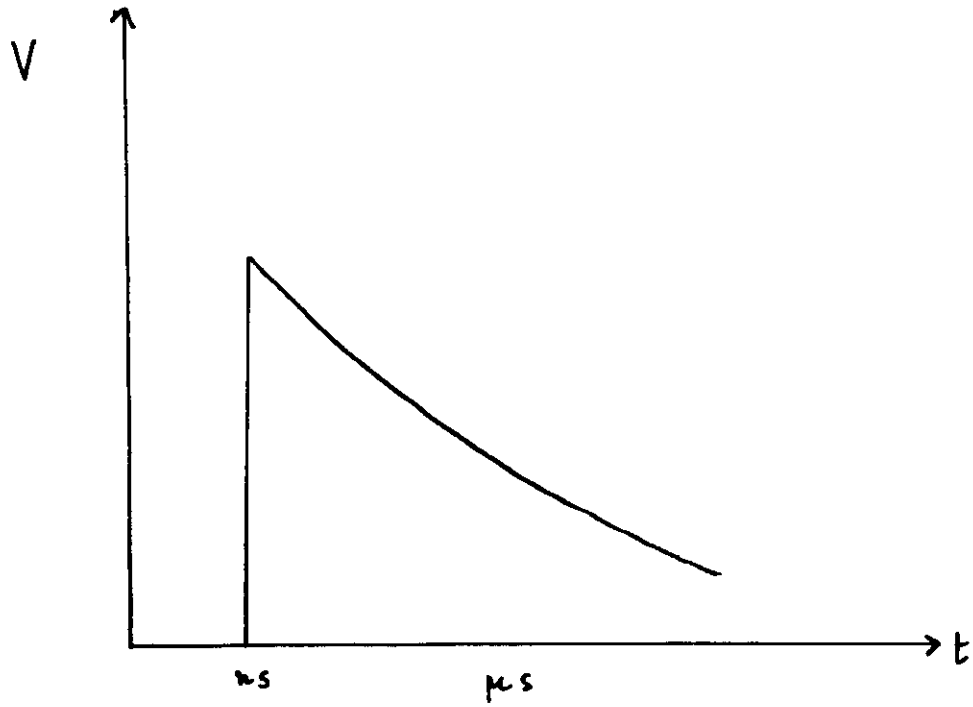

Figure 6.2 - Typical pulse shape of a nuclear detector.

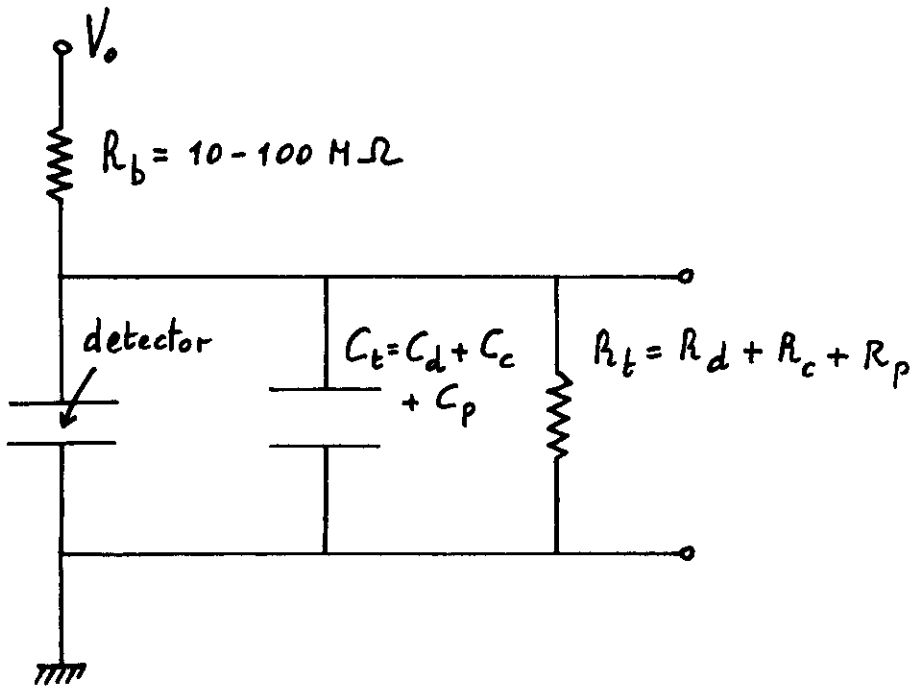

Figure 6.3 - Electronic circuit of a detector.

C_d = detector capacitance

C_c = connectors and cables capacitance

C_p = parasite capacitance

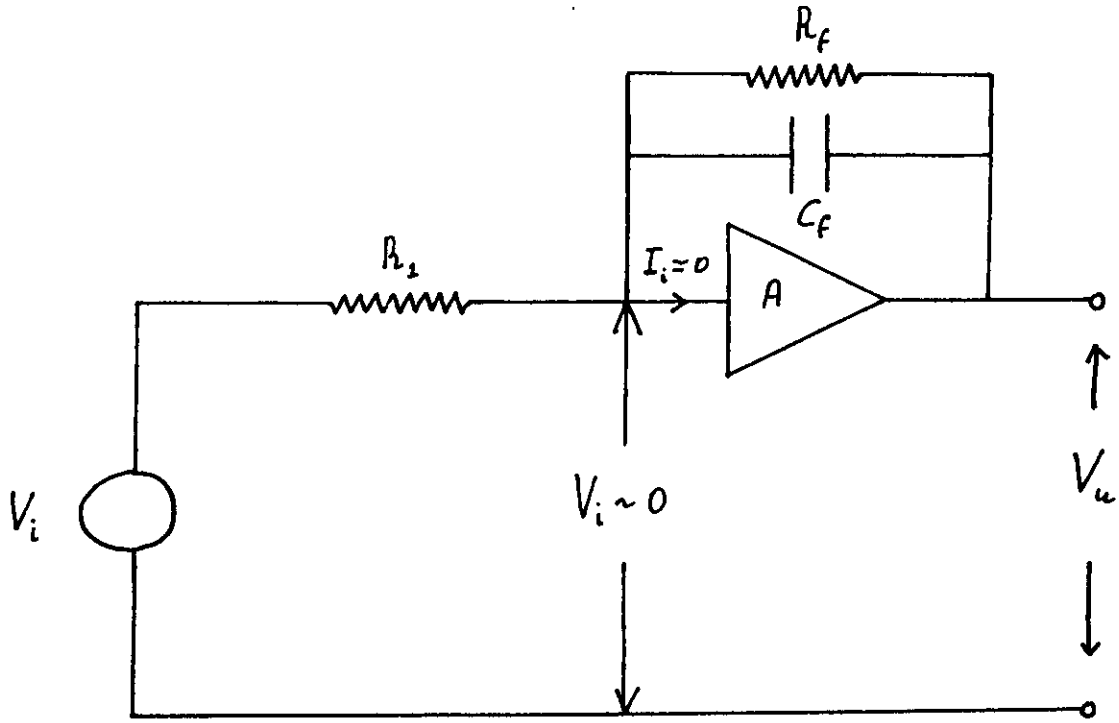

Figure 6.4 - Coupling of a charge sensitive preamplifier with feedback to a detector.

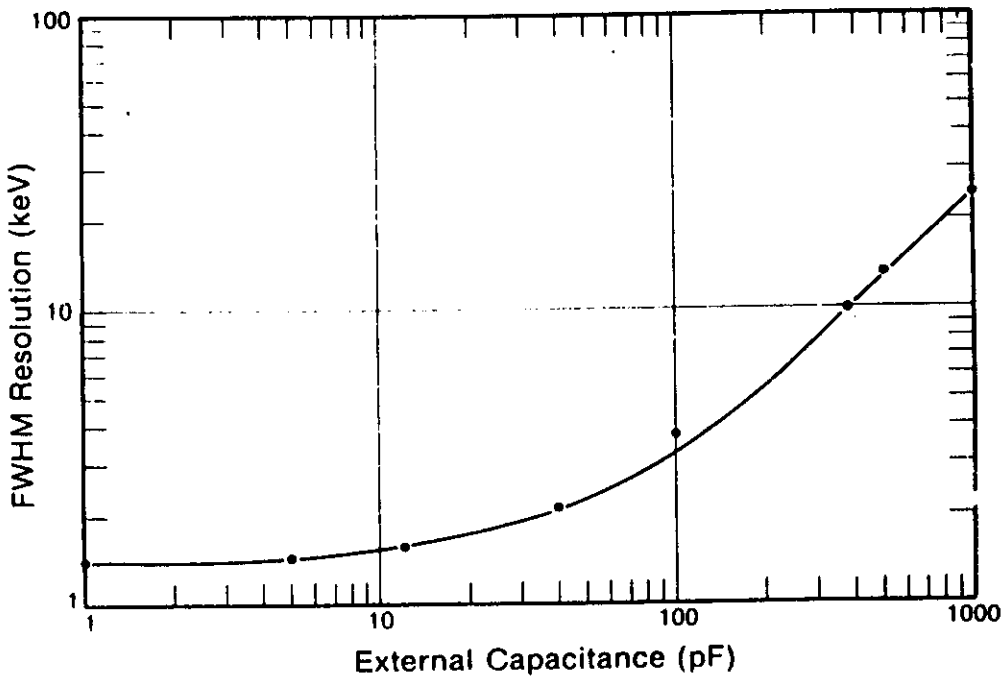

Figure 6.5 - Noise vs. external capacitance for a typical preamplifier.

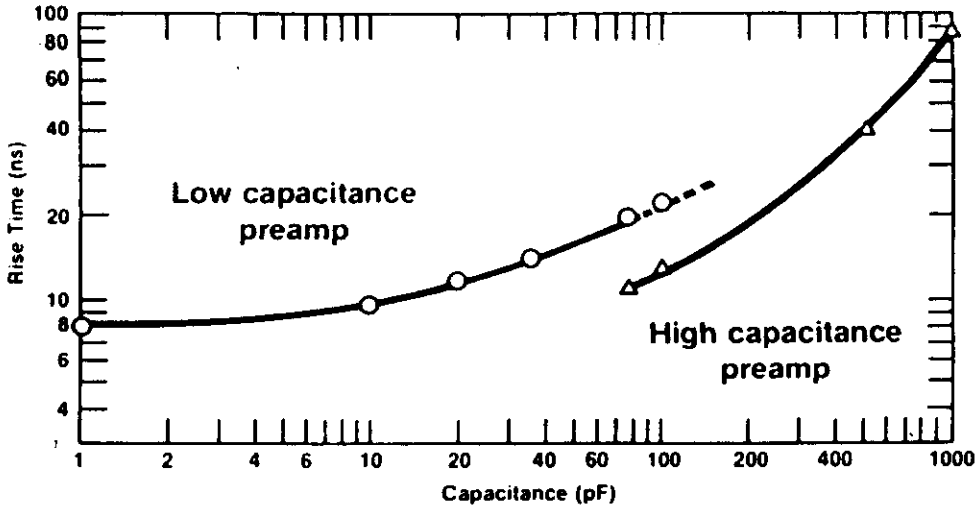

Figure 6.6 - Output rise time of a charge-sensitive preamplifier vs. external capacitance.

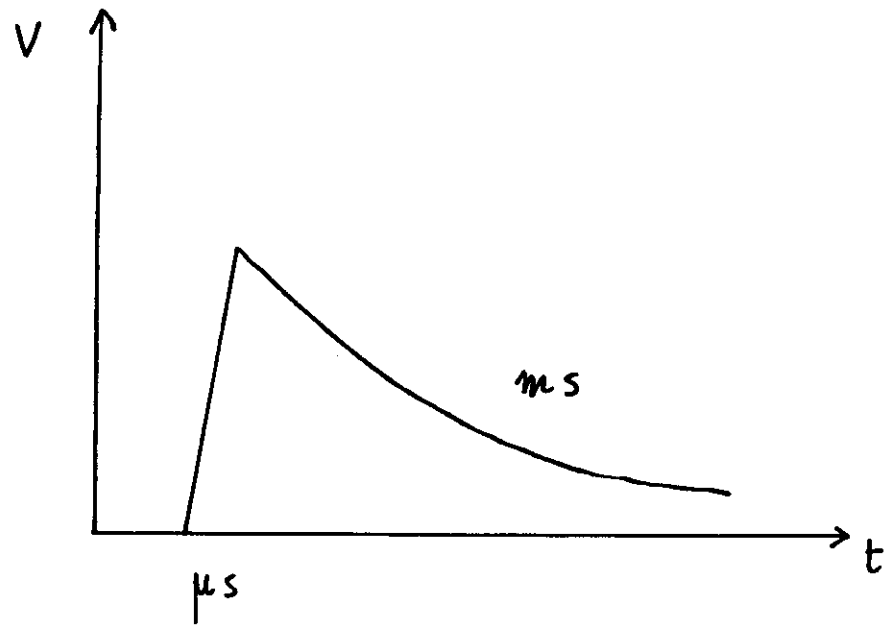

Figure 6.7 - Preamplifier output signal.

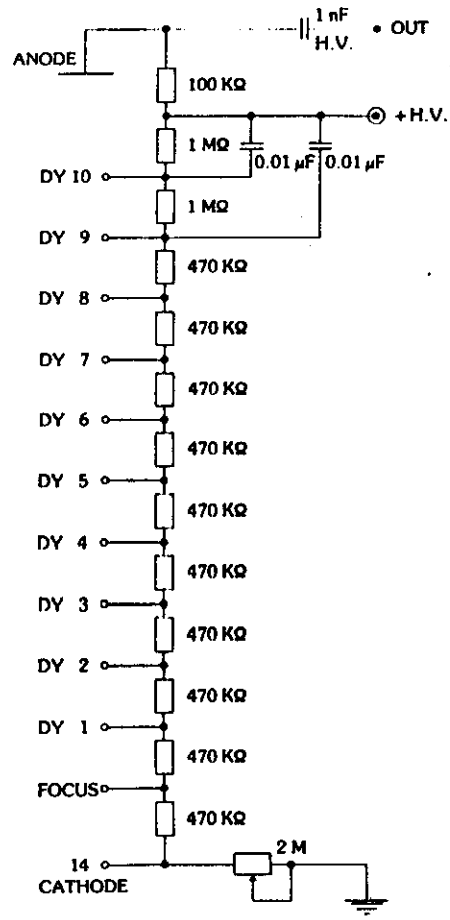

Figure 6.8 - Standard voltage divider network for a 10 dynodes photomultiplier.

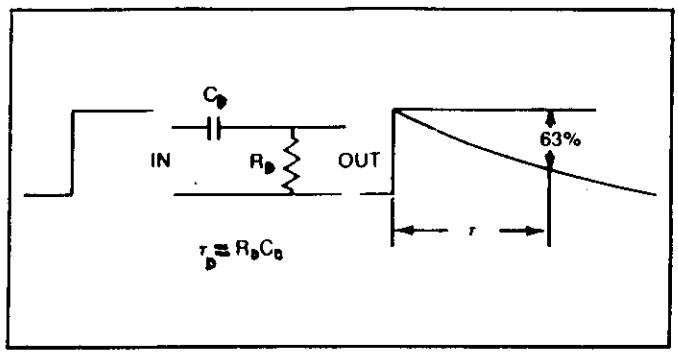

Figure 6.9 - CR-differentiation filter

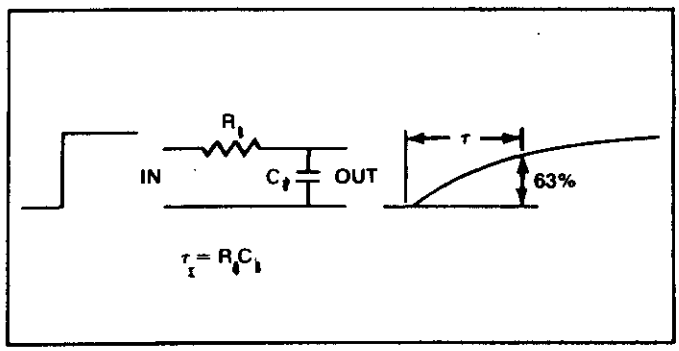

Figure 6.10 - RC-integration filter.

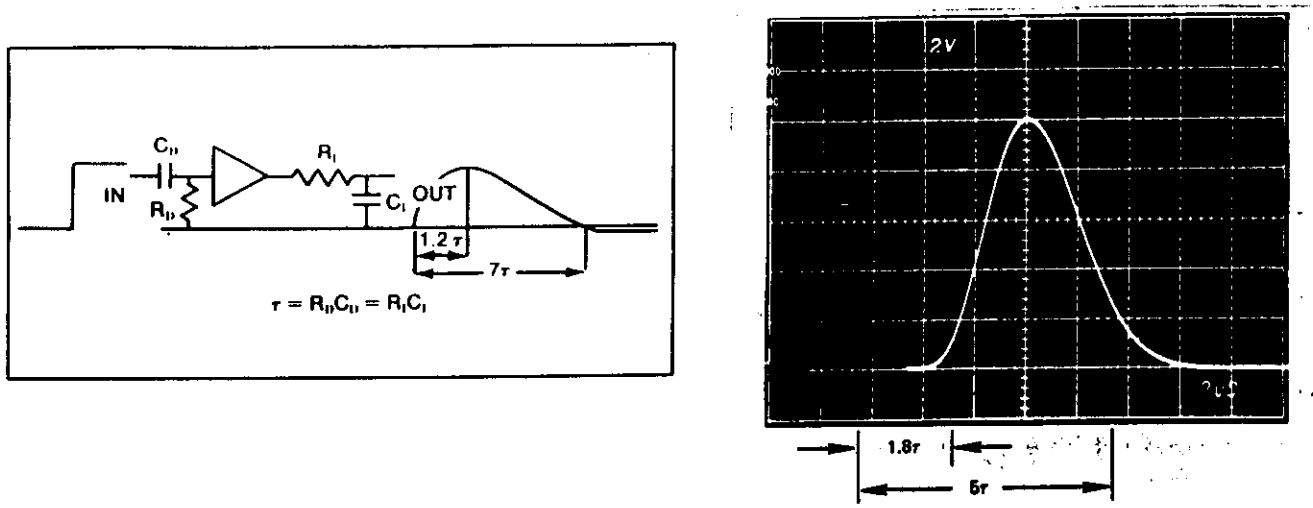

Figure 6.11 - CR-RC- unipolar pulse shaping.

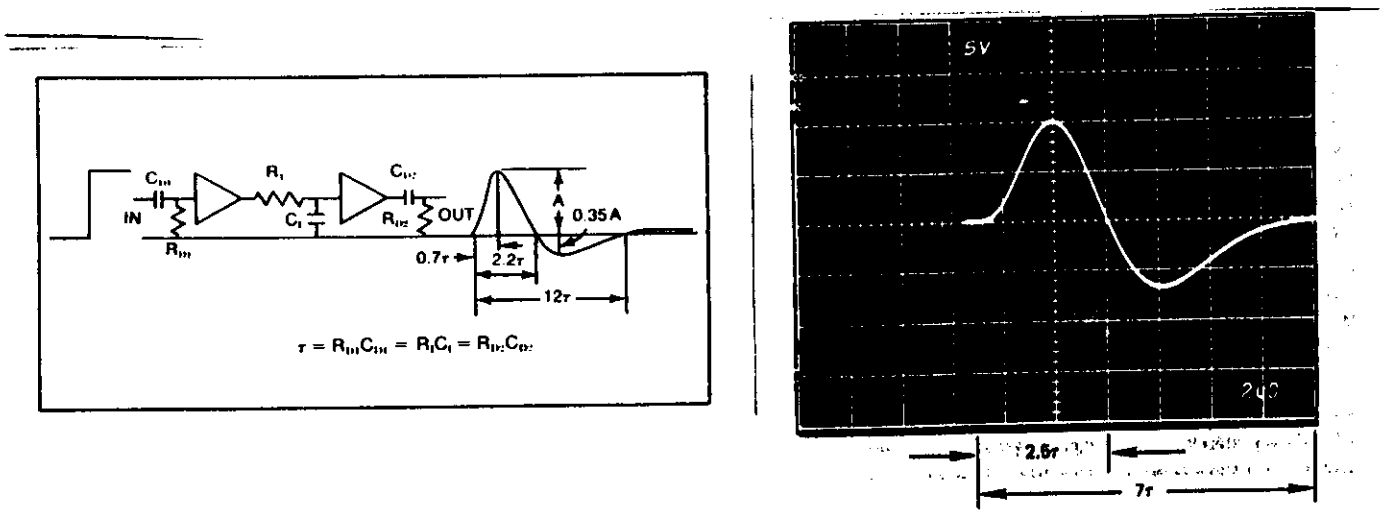

Figure 6.12 - CR-RC-CR-bipolar pulse shaping.

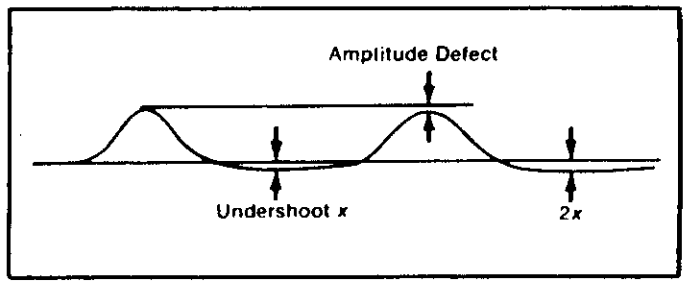

Figure 6.13 - Pulse distortion of unipolar pulses due to the undershoot.

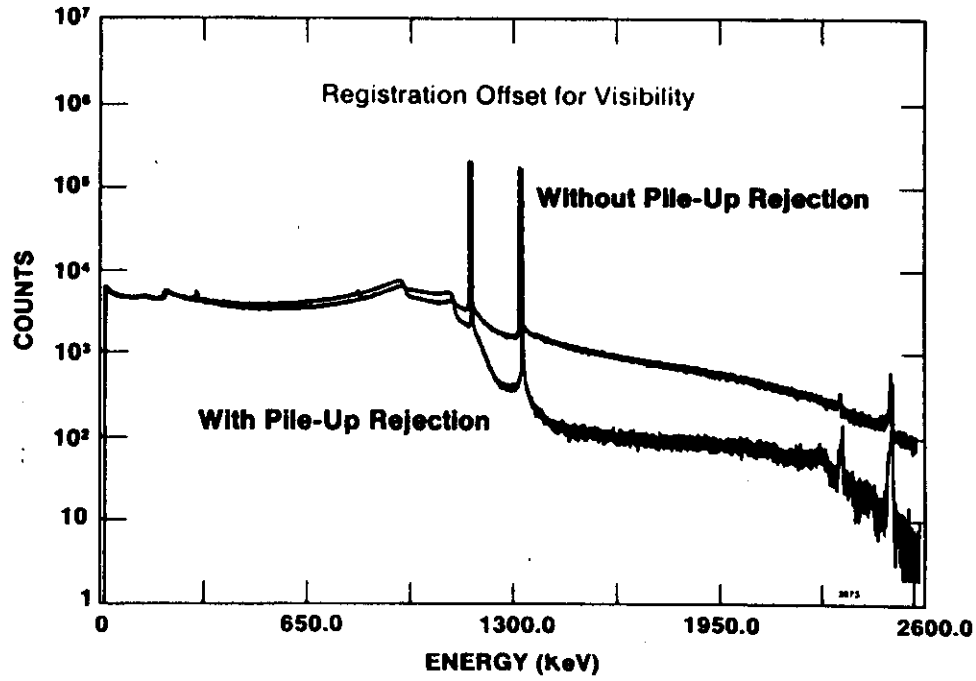

Figure 6.14 - Background reduction in a gamma-ray spectrum as pileup rejection is used.

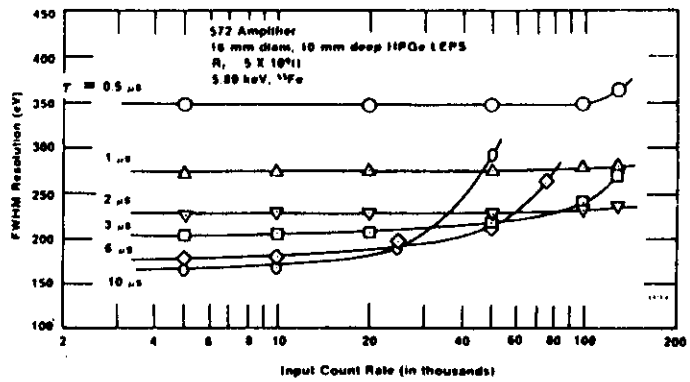

Figure 6.15 - Energy resolution of a planar HPGe detector versus feedback resistor.

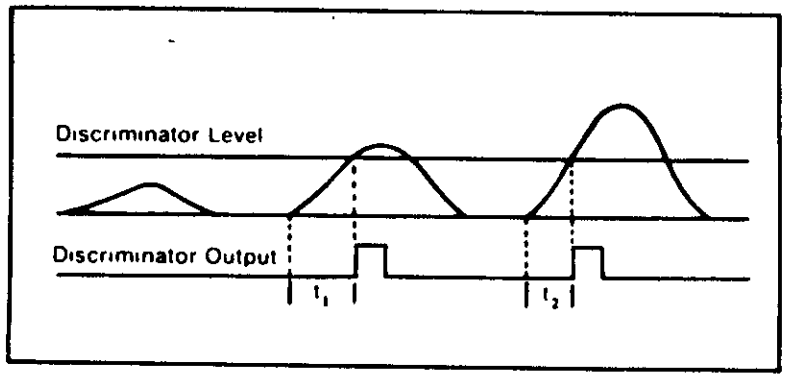

Energy 6.16 - Integral discriminator

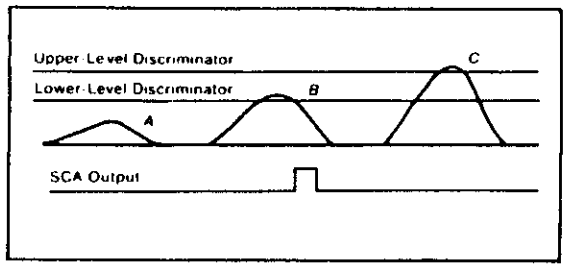

Figure 6.17 - Selection of pulses by a single-channel-analyzer.

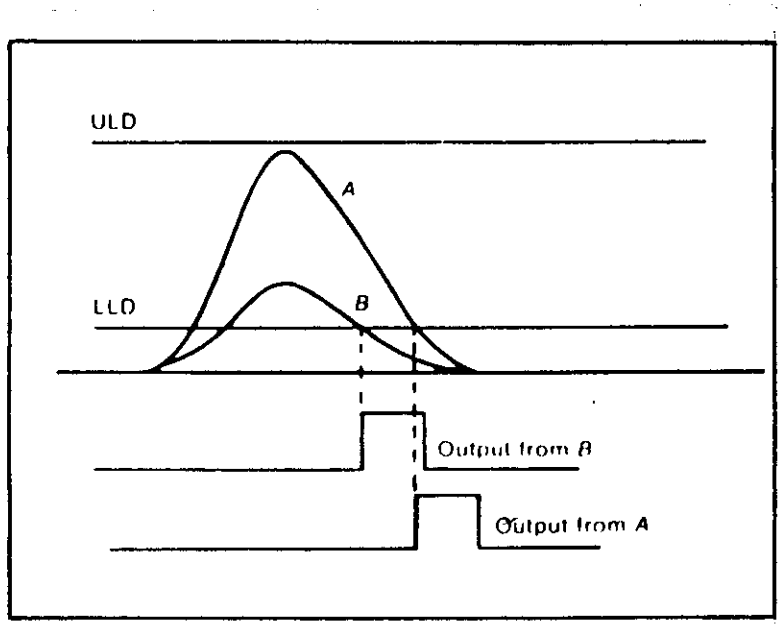

Figure 6.18 - Time response of a SCA for two unipolar pulses from the amplifier.

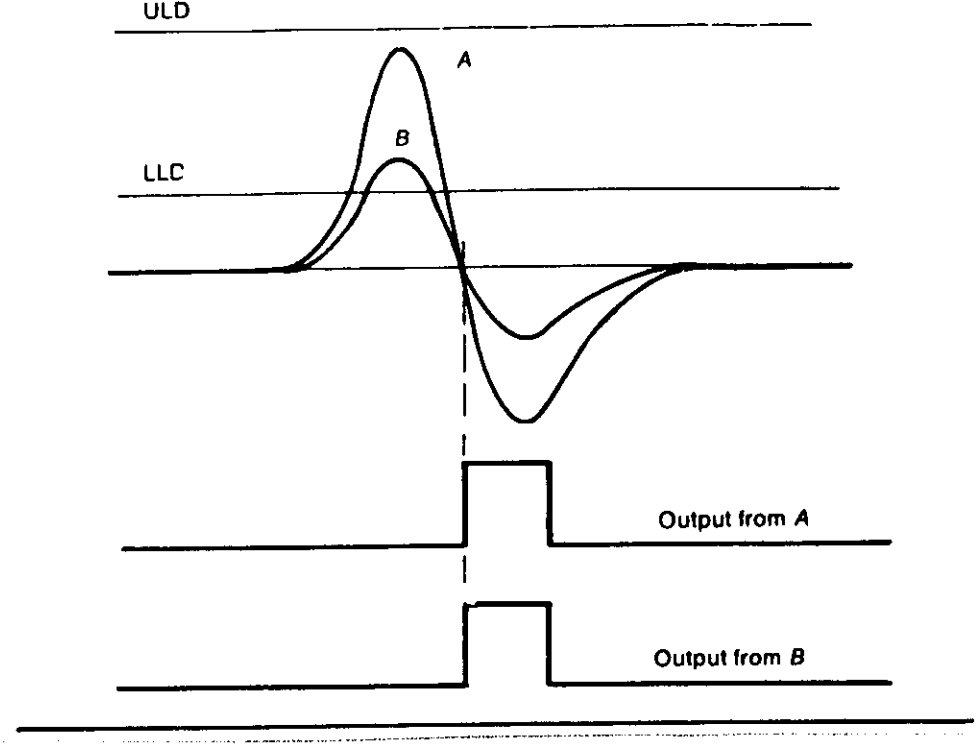

Figure 6.19 - Time-response of a SCA for two bipolar pulses from an amplifier.

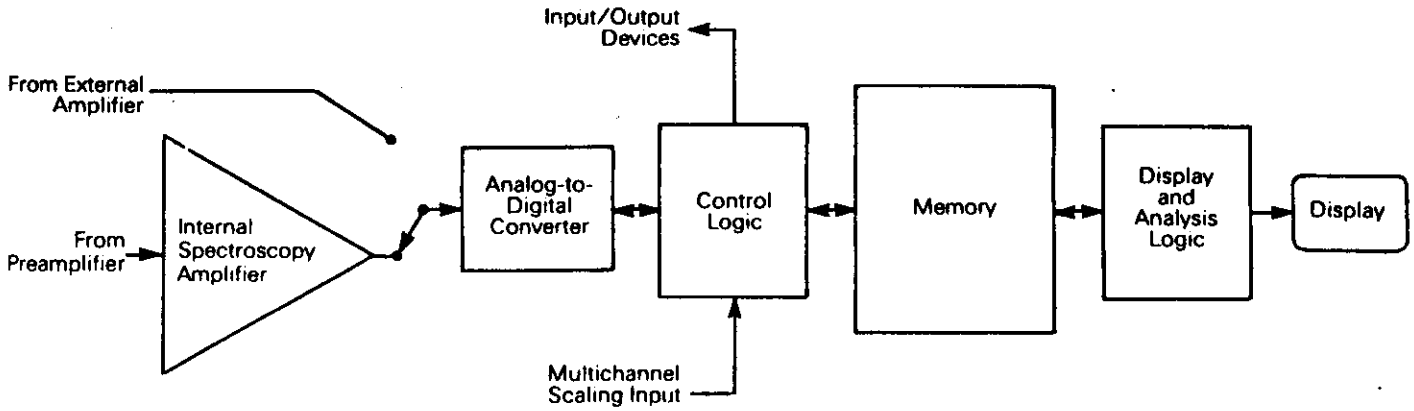

Figure 6.20 - Block diagram of a multi-channel-analyzer.

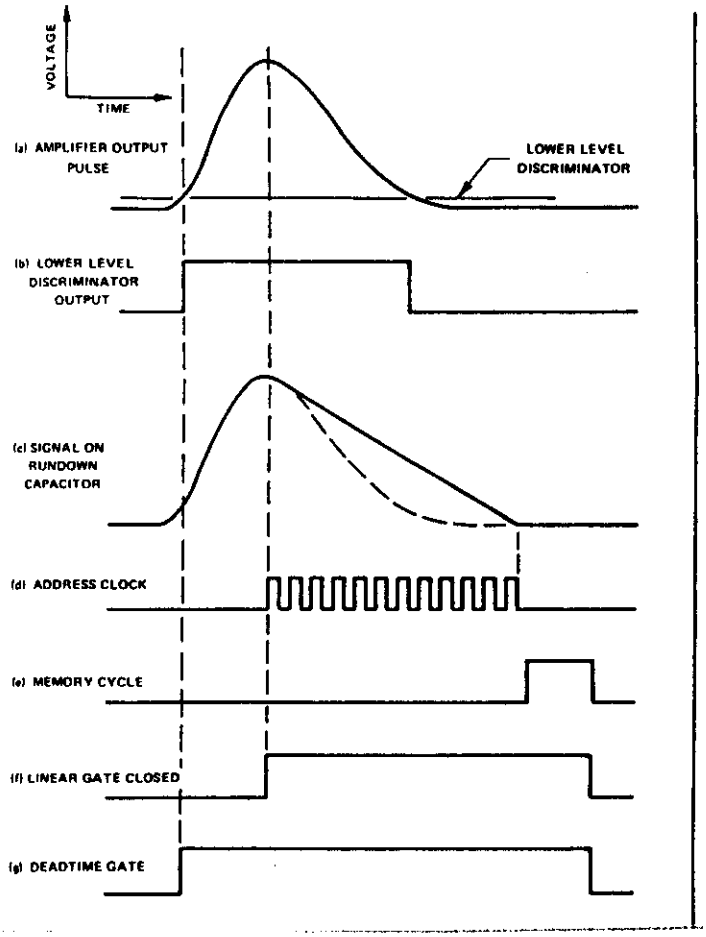

Figure 6.21 - Signals in the Wilkinson ADC during the pulse measurement process.

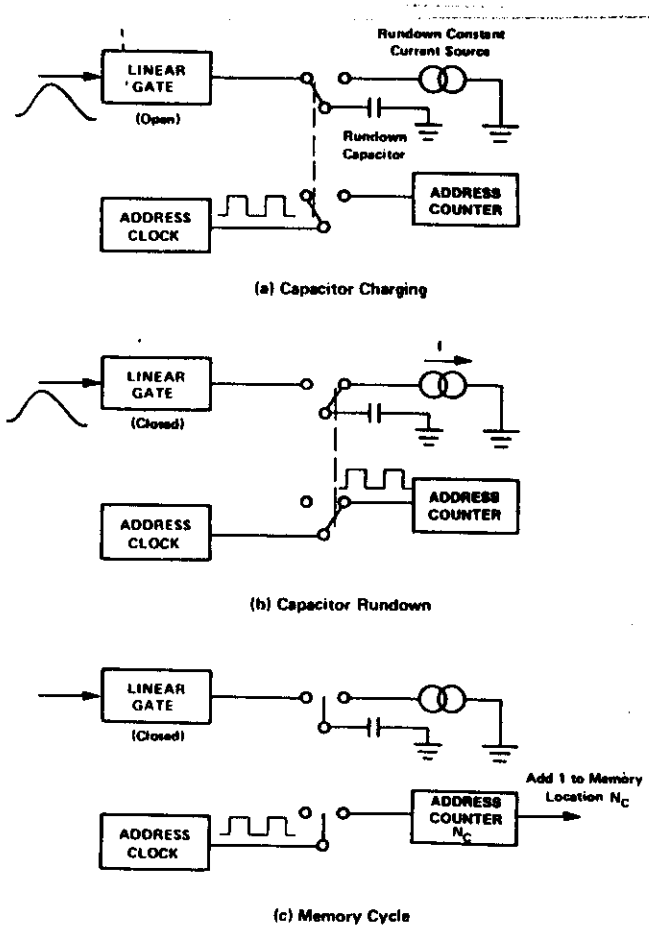

Figure 6.22 - Operation of the Wilkinson ADC during the three stages of pulse amplitude measurement: a) charging of the

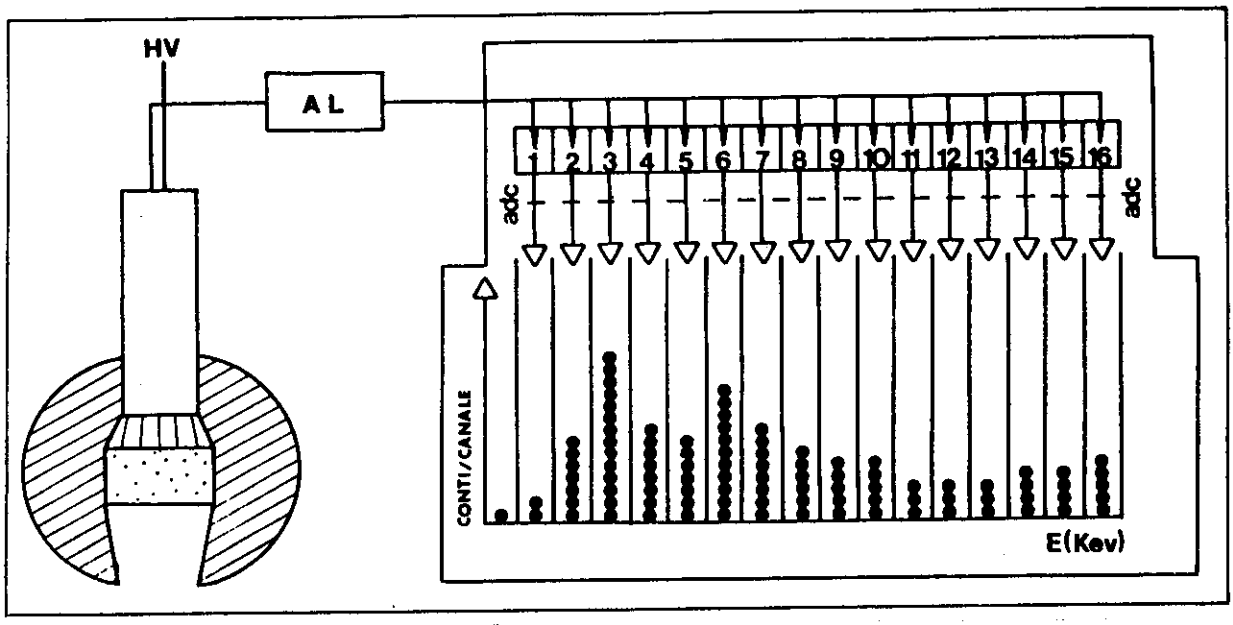

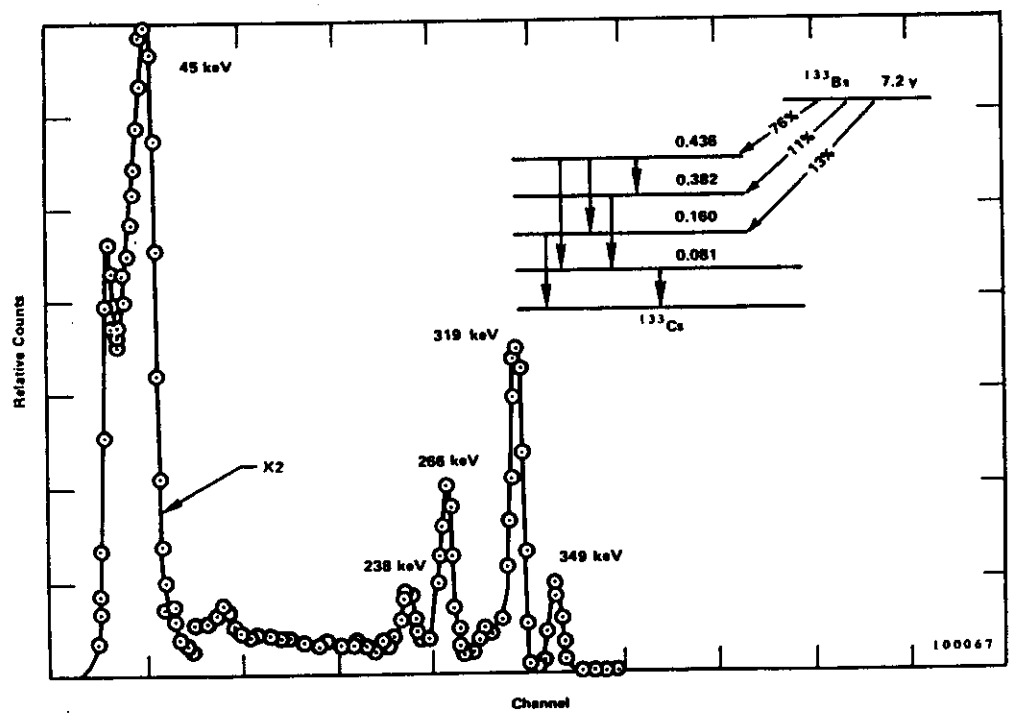

Figure 6.23 Hystogram or "spectrum" of a nuclear process.

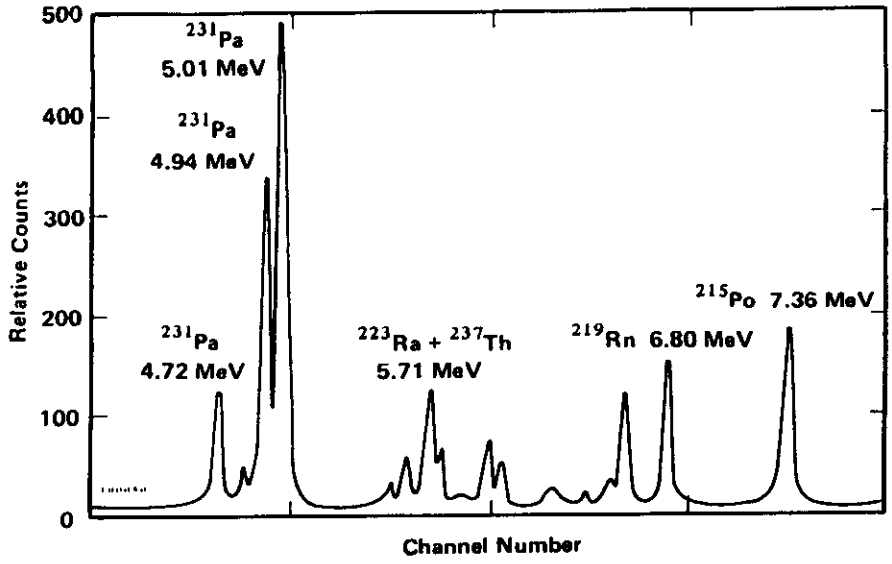

Figure 7.1 - alpha spectrum of Th^{232}

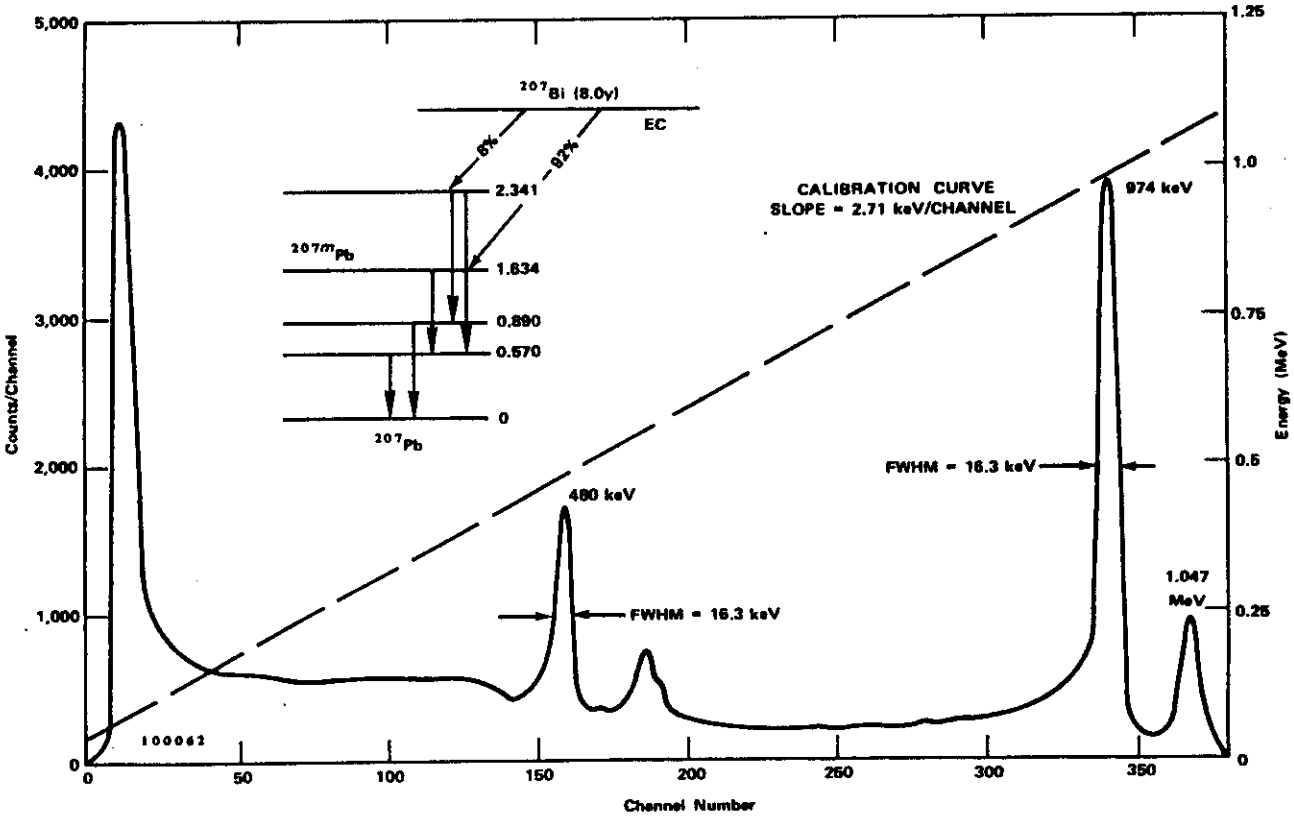

Figure 7.2 - Beta spectrum of Bi^{207}.

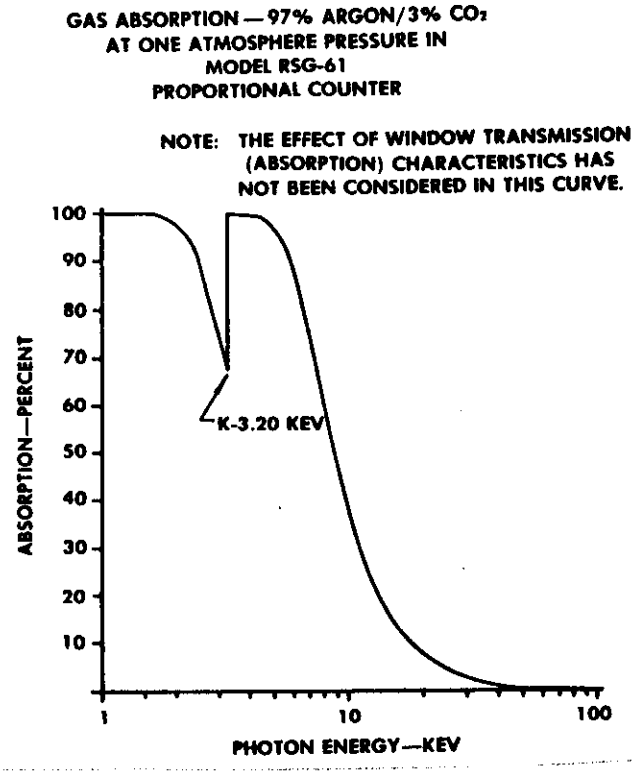

Figure 7.3 - Absorption curve of argon at 1 atm.

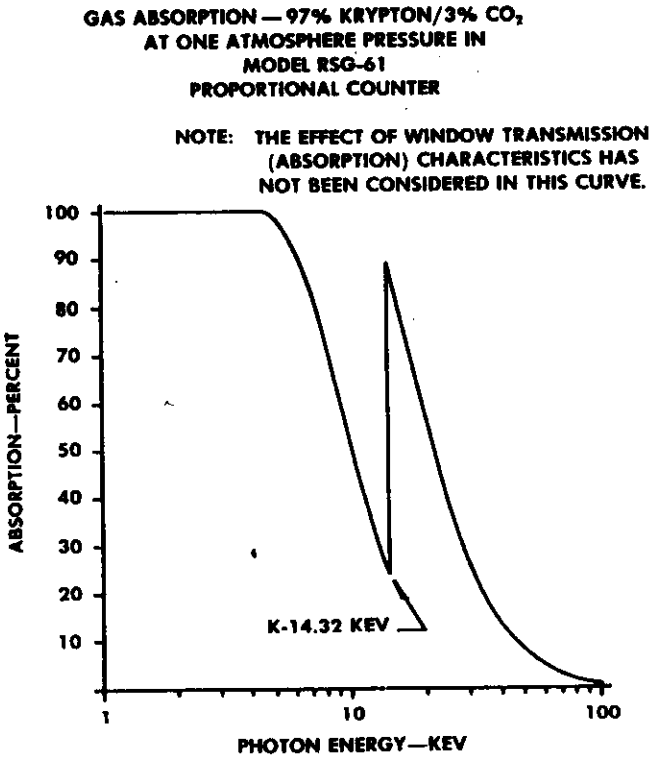

Figure 7.4 - Absorption curve of krypton at 1 atm.

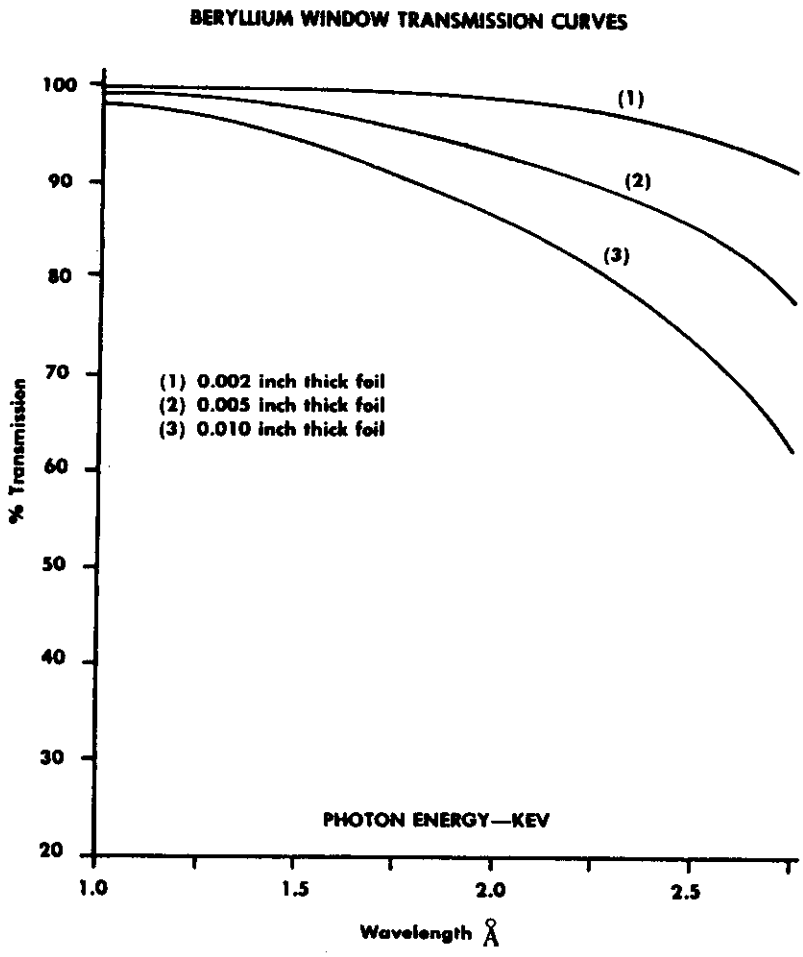

Figure 7.5 - Window transmission for a gas proportional counter

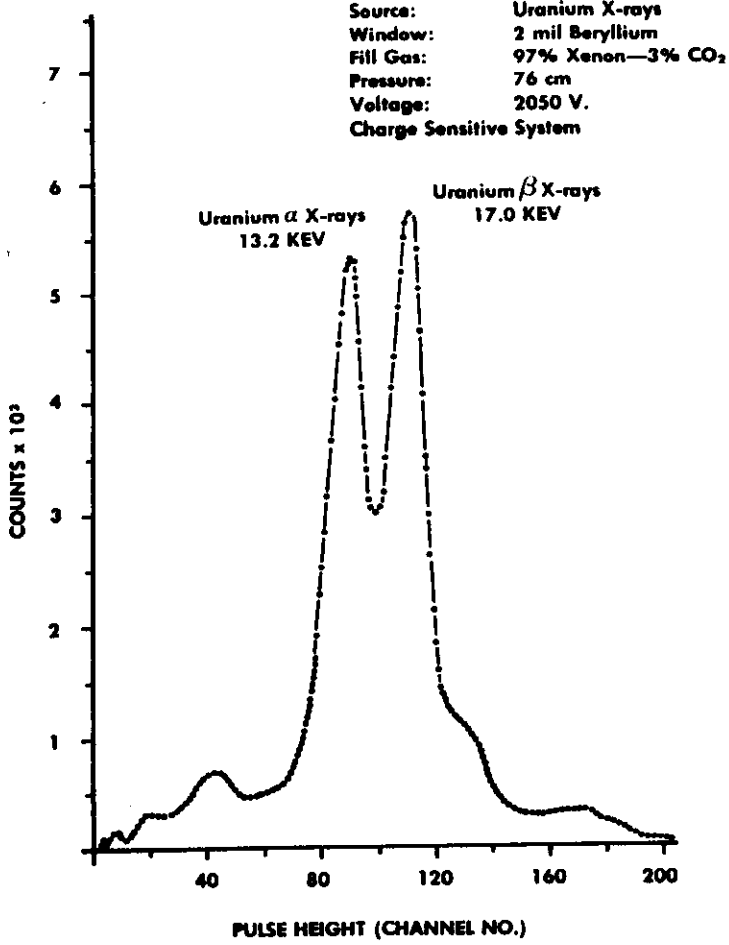

Figure 7.6 - Spectrum of a xenon-filled gas proportional counter

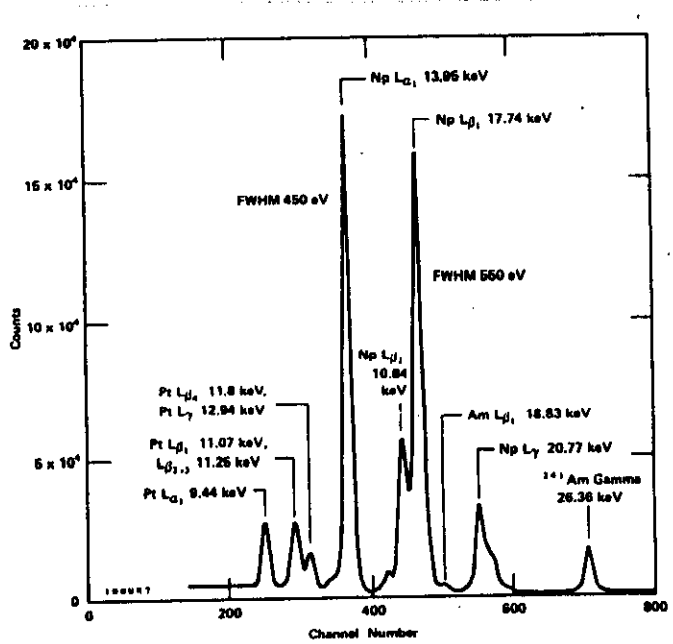

Figure 7.7 - Typical X-ray spectrum collected with a semiconductor detector

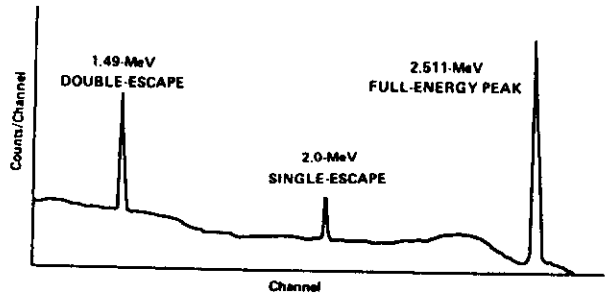

Figure 7.8 - Typical gamma-ray spectrum showing the full-energy, single-escape and double escape peaks.

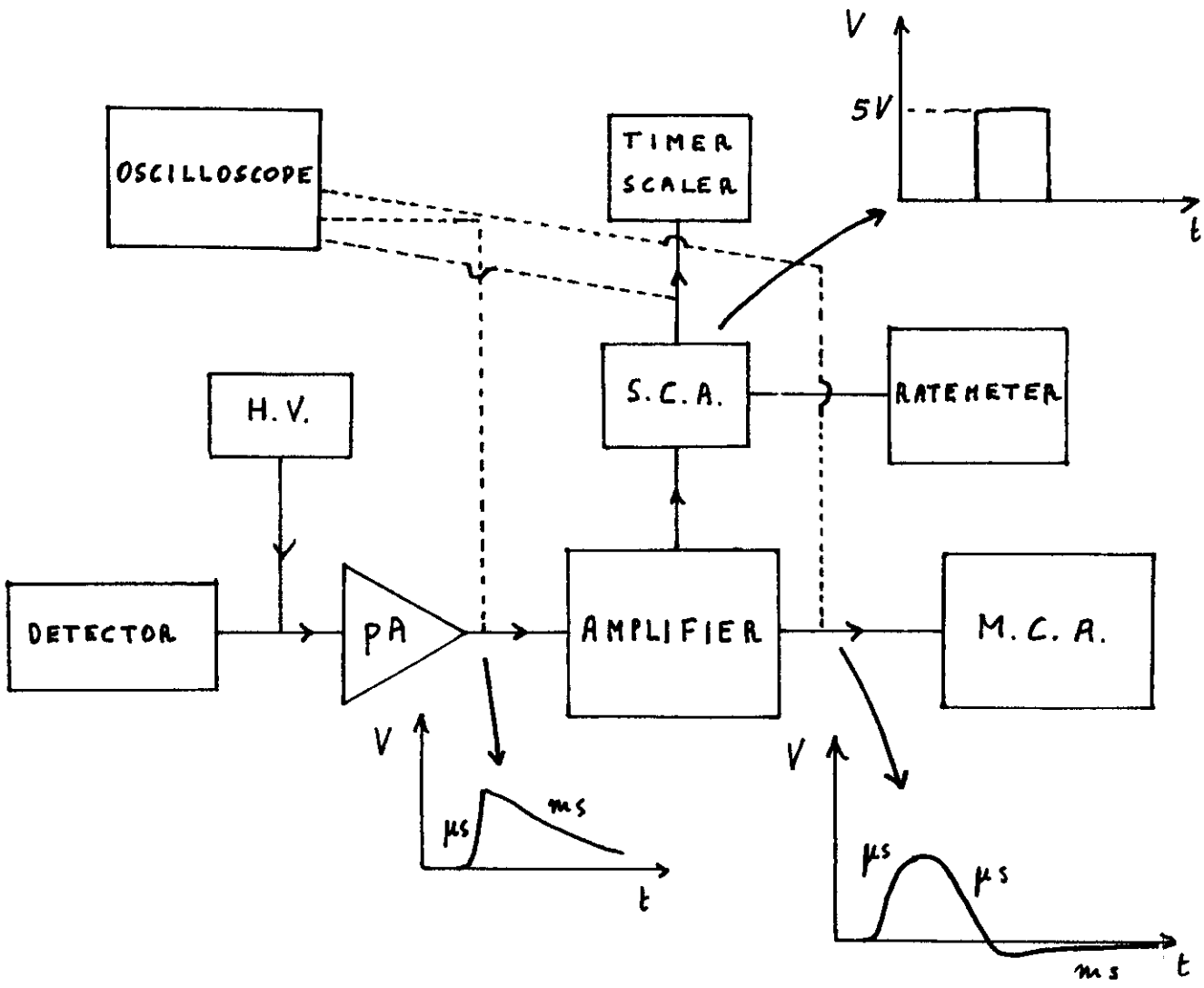

Figure 8.1 - Use of an oscilloscope in a nuclear electronic chain.